

Electrochemical reduction of CO₂ to CO on Zn electrodes
prepared by electrodeposition method



A Thesis Submitted in Partial Fulfillment of the Requirements
for the Degree of Master of Engineering in Chemical Engineering
Department of Chemical Engineering
FACULTY OF ENGINEERING
Chulalongkorn University
Academic Year 2020
Copyright of Chulalongkorn University

การรีดักชันทางเคมีไฟฟ้าของแก๊สคาร์บอนไดออกไซด์เป็นแก๊สคาร์บอนมอนอกไซด์บน
อิเล็กโทรดสังกะสีที่เตรียมโดยวิธีการพอกพูนทางไฟฟ้า



วิทยานิพนธ์นี้เป็นส่วนหนึ่งของการศึกษาตามหลักสูตรปริญญาวิศวกรรมศาสตรมหาบัณฑิต
สาขาวิชาวิศวกรรมเคมี ภาควิชาวิศวกรรมเคมี
คณะวิศวกรรมศาสตร์ จุฬาลงกรณ์มหาวิทยาลัย
ปีการศึกษา 2563
ลิขสิทธิ์ของจุฬาลงกรณ์มหาวิทยาลัย

ครองขวัญ พูลบุญ : การรีดักชันทางเคมีไฟฟ้าของแก๊สคาร์บอนไดออกไซด์เป็นแก๊สคาร์บอนมอนอกไซด์บนอิเล็กโทรดสังกะสีที่เตรียมโดยวิธีการพอกพูนทางไฟฟ้า. (Electrochemical reduction of CO₂ to CO on Zn electrodes prepared by electrodeposition method)
 อ.ที่ปรึกษาหลัก : ศ. ดร.จุงใจ ปั้นประณต

ในงานนี้ศึกษาอิทธิพลของตัวรองรับได้แก่แผ่นทองแดงและแผ่นไทเทเนียมสำหรับตัวเร่งปฏิกิริยาสังกะสีที่เตรียมโดยวิธีการพอกพูนทางไฟฟ้าต่อความสามารถในการเร่งปฏิกิริยาในปฏิกิริยารีดักชันแบบใช้ไฟฟ้าช่วยของคาร์บอนไดออกไซด์ ผลจากเทคนิคกล้องจุลทรรศน์อิเล็กตรอนแบบส่องกราดร่วมกับเอ็กซ์เรย์สเปกโตรสโกปีแบบกระจายพลังงาน และการกระเจิงของรังสีเอ็กซ์แสดงให้เห็นว่าการใช้ตัวรองรับที่ต่างกันไม่ได้ส่งผลต่อรูปร่างของสังกะสีโดยพบว่าการนำไฟฟ้าของตัวรองรับเป็นปัจจัยหลักที่ส่งต่อสมรรถนะในปฏิกิริยารีดักชันแบบใช้ไฟฟ้าช่วยของคาร์บอนไดออกไซด์ สำหรับการศึกษาผลของความเข้มข้นของสังกะสีในช่วง 0.025 โมลาร์ ถึง 0.4 โมลาร์ต่อคุณลักษณะและความสามารถในการเร่งปฏิกิริยารีดักชันแบบใช้ไฟฟ้าช่วยของคาร์บอนไดออกไซด์ของตัวเร่งปฏิกิริยาสังกะสีบนแผ่นทองแดง พบว่าที่ความเข้มข้นเจือจางของสังกะสี (0.025 โมลาร์และ 0.05 โมลาร์) ได้รูปร่างเด่นโดเร่ที่เหมือนกันและเมื่อเพิ่มความเข้มข้นของสังกะสีที่ 0.1 โมลาร์ รูปร่างเปลี่ยนเป็นลักษณะที่เรียกว่าซิงค์มอสซีโดยมีปริมาณสังกะสีเกาะติดมากที่สุด และหากความเข้มข้นของสังกะสีมากกว่า 0.1 โมลาร์ ปริมาณสังกะสีเกาะติดจะลดลงเนื่องจากอัตราการเกิดปฏิกิริยาแข่งขันของการเกิดไฮโดรเจนมากขึ้นและยังทำให้พบการเกิดออกไซด์บนพื้นผิวของผิวสังกะสีปริมาณมากซึ่งจะไปขัดขวางในปฏิกิริยารีดักชันแบบใช้ไฟฟ้าช่วยของคาร์บอนไดออกไซด์ จากตัวเร่งปฏิกิริยาทั้งหมดในงานนี้พบว่าตัวเร่งปฏิกิริยาที่ให้ประสิทธิภาพทางไฟฟ้าของการเกิดแก๊สคาร์บอนมอนอกไซด์มากที่สุดคือ 0.05สังกะสี/ทองแดง ทั้งนี้อาจเนื่องมาจากการเกิดปริมาณผลิตภัณฑ์สังกะสีระนาบ(101) ที่ว่องไวต่อปฏิกิริยามากที่สุด สำหรับการศึกษาการใช้งานตัวเร่งปฏิกิริยา 0.05สังกะสี/ทองแดง ในปฏิกิริยารีดักชันแบบใช้ไฟฟ้าช่วยของคาร์บอนไดออกไซด์ในอิเล็กโทรไลต์แบบสารละลายน้ำและในของเหลวไอออนิก พบว่าของเหลวไอออนิกช่วยลดค่าศักย์ไฟฟ้าที่ใช้เกิดปฏิกิริยาได้แต่ตัวเร่งปฏิกิริยาในของเหลวไอออนิกนั้นไม่เสถียรจึงเกิดการหลุดออกจากพื้นผิว ในทางตรงข้ามตัวเร่งปฏิกิริยาในสารละลายน้ำสามารถเกิดการกลับมาเกาะใหม่ ของสังกะสีบนตัวรองรับจึงทำให้ประสิทธิภาพทางไฟฟ้าของการเกิดแก๊สคาร์บอนมอนอกไซด์มากที่สุด นอกจากนี้ 0.05สังกะสี/ทองแดงยังให้ค่าประสิทธิภาพทางไฟฟ้าของการเกิดแก๊สคาร์บอนมอนอกไซด์มากกว่าแผ่นสังกะสีประมาณ 1.5 เท่า ซึ่งแสดงให้เห็นถึงโครงสร้างเด่นโดเร่ที่ช่วยส่งเสริมความสามารถในการเร่งปฏิกิริยาของแก๊สคาร์บอนไดออกไซด์

สาขาวิชา วิศวกรรมเคมี

ลายมือชื่อนิสิต

ปีการศึกษา 2563

ลายมือชื่อ อ.ที่ปรึกษาหลัก

6270025621 : MAJOR CHEMICAL ENGINEERING

KEYWORD: Electrochemical carbon dioxide reduction, Carbon monoxide production, Electrodeposition, Zinc catalyst

Krongkwan Poonbun : Electrochemical reduction of CO₂ to CO on Zn electrodes prepared by electrodeposition method. Advisor: Prof. JOONGJAI PANPRANOT, Ph.D.

In this work, the effect of substrates including Cu and Ti on the catalytic activity of Zn electrocatalysts prepared by electrodeposition method was investigated in the electrochemical reduction of CO₂ (CO₂ER). As analyzed by SEM-EDX and XRD results, it indicated that the different substrates did not have any influence on the morphologies of catalysts and the conductivity of substrate was the main factor on the CO₂ER performance. The effect of Zn precursor concentration in the range of 0.025 M to 0.4 M was further studied on the characteristics and the activity of Zn/Cu catalysts in the CO₂ER. At low concentrations of Zn precursor (0.025M and 0.05M), the catalysts exhibited the same dendrite structure. Increasing Zn concentration to 0.1 M, the morphology changed into mossy structure with the highest amount of Zn deposited. On the contrary, at higher concentration of Zn precursor than 0.1M, lower amount of Zn was deposited because of the faster H₂ evolution rate. In addition, larger amount of oxide layer was covered on Zn surface, which impeded the performances of the CO₂ER. Among the prepared catalysts, the best catalyst was 0.05 Zn/Cu, which provided the highest faradaic efficiency (FE) of CO due probably to the highest amount of catalytic active Zn (101) facet. Finally, comparing the use of 0.05Zn/Cu electrocatalysts in aqueous electrolyte and ionic liquid, the results showed that ionic liquid decreased the applied potential in the CO₂ER but the Zn catalyst was not stable and then, fell off the catalyst surface. In contrast, the Zn catalyst in aqueous solution could re-deposit on the substrate after CO₂ER. The highest %FE of CO was achieved in 0.1 M KHCO₃. Moreover, 0.05Zn/Cu provided the nearly 1.5 times higher %FE of CO than Zn foil, indicating that the dendrite structure enhanced the CO₂ER activity.

จุฬาลงกรณ์มหาวิทยาลัย
CHULALONGKORN UNIVERSITY

Field of Study: Chemical Engineering

Student's Signature

Academic Year: 2020

Advisor's Signature

ACKNOWLEDGEMENTS

I am much admired my advisor, Prof. Dr. Joongjai Panpranot. She has provided advice, counselling, assistance, and motivation for my thesis since start to first study until last semester to prepare thesis's defense exam, Besides, I am appreciative to Asst. Prof. Dr. Amornchai Arpornwichanop, as the chairman, Dr. Chutimon Satirapipathkul and Dr. Patcharaporn Weerachawanasak as an examiner of the committee group for their significant guidance and recommendation on this thesis.

Moreover, I am impressed to my parents and my friends for give me a helpful and many valuable suggestions when I faced with stress and many problems.

The financial help obtaining from The Malaysia-Thailand Joint Authority (MTJA) is extremely notable.

Krongkwan Poonbun

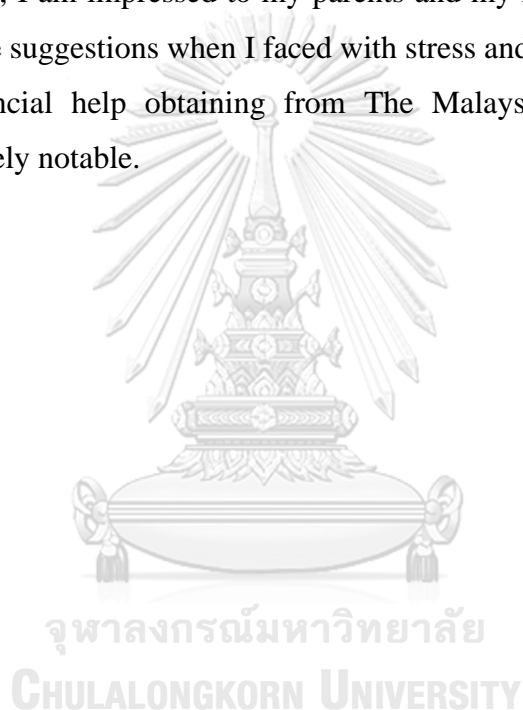


TABLE OF CONTENTS

	Page
ABSTRACT (THAI)	iii
ABSTRACT (ENGLISH).....	iv
ACKNOWLEDGEMENTS	v
TABLE OF CONTENTS.....	vi
LIST OF TABLES	viii
LIST OF FIGURES	ix
CHAPTER I INTRODUCTION.....	1
1.1 Introduction	1
1.2 Objectives of the Research	2
1.3 Scopes of the Research	3
CHAPTER II BACKGROUND AND LITERATURE REVIEWS.....	4
2.1 Fundamental of electrochemical reduction of CO ₂	4
2.2 Study on electrodes.....	5
2.3 Electrodeposition of Zn electrocatalysts.	9
2.4 Ionic liquids (ILs).....	15
CHAPTER III MATERIALS AND METHODS	19
3.1 Materials	19
3.2 Catalysts preparation	20
3.2.1 Preparation of electrodes.....	20
3.2.2 Preparation of Zn catalysts.....	20
3.3 Catalyst Characterization.....	21
3.3.1 Scanning electron microscope-energy dispersive X-ray spectroscopy (SEM-EDX)	21
3.3.2 X-ray diffraction (XRD).....	22
3.4 Electrochemical CO ₂ reduction	22
3.5 Research methodology	25

CHAPTER IV RESULTS AND DISCUSSION.....	28
4.1 Characterization of Zn electrocatalysts on different substrates (Cu, Ti).....	28
4.1.1 Scanning electron microscope-energy dispersive X-ray spectroscopy (SEM-EDX) of 0.05Zn/Cu and 0.05Zn/Ti	28
4.1.2 X-ray diffraction (XRD) of 0.05Zn/Cu and 0.05Zn/Ti	30
4.2 Activity test of Zn electrocatalysts on different substrates (Cu, Ti) in the CO ₂ ER	31
4.3 Characterization of Zn foil, Cu foil and Zn/Cu prepared with various Zn concentrations.....	33
4.3.1 Scanning electron microscope-energy dispersive X-ray spectroscopy (SEM-EDX) of Zn foil, Cu foil, and Zn/Cu at various concentrations	33
4.3.2 X-ray diffraction (XRD) of Zn foil, Cu foil, and Zn/Cu at various concentrations.....	39
4.4 Activity test of Zn electrocatalysts of Zn foil, Cu foil and Zn/Cu prepared with various Zn concentrations.....	40
4.5 Electrochemical measurement of 0.05Zn/Cu in 0.1 M KHCO ₃ and ionic liquid (PC/[BMIM]BF ₄).....	42
4.5.1 Linear sweep voltammetry (LSV) of 0.05Zn/Cu in 0.1 M KHCO ₃ and ionic liquid (IL)	42
4.5.2 Comparison of the activity tests of 0.05Zn/Cu in 0.1 M KHCO ₃ and IL.	43
CHAPTER V CONCLUSIONS	47
5.1 Conclusions	47
5.2 Recommendations	48
REFERENCES	49
APPENDIX.....	55
VITA.....	60

LIST OF TABLES

Table 1. Standard electrochemical potentials for CO ₂ reduction.....	4
Table 2. Sn-based electrode in the CO ₂ ER.	6
Table 3. Au-based electrode in the CO ₂ ER.	7
Table 4. Ag-based electrode in the CO ₂ ER.	7
Table 5. Zn-based electrode in the CO ₂ ER.....	8
Table 6. Cu-based electrode in the CO ₂ ER.....	8
Table 7. Zn electrocatalysts by electrodeposition method.....	11
Table 8. Comparison between the advantages and the disadvantages in various solutions [29, 77, 78]	16
Table 9. Chemicals used as precursors and electrolyte.....	19
Table 10. Metals used as electrodes in electrodeposition method and electrochemical reduction of CO ₂	19
Table 11. The operating conditions of gas chromatograph with a thermal conductivity detector.....	24
Table 12. Percent by atom of 0.05Zn/Cu and 0.05Zn/Ti.	29
Table 13. The catalytic performances of Zn/Cu and Zn/Ti.	31
Table 14. Percent by atom of Zn/Cu at various concentrations.....	37
Table 15. The catalytic performances of Zn foil, Cu foil and Zn/Cu prepared with various Zn concentrations.	40
Table 16. The catalytic performances of 0.05Zn/Cu in 0.1 M KHCO ₃ and IL.	43
Table 17. Percent by atom of 0.05Zn/Cu after run reaction in 0.1M KHCO ₃ and IL.	45

LIST OF FIGURES

Figure 1. Possible pathways for CO ₂ ER on metal surfaces in aqueous solution [40].	6
Figure 2. Diagram of steps in the cathodic deposition of metals.	10
Figure 3. Cations and anions in ILs used the CO ₂ ER.	17
Figure 4. Schematic of electrodeposition of Zn catalysts on different substrates.	21
Figure 5. Schematic of electrodeposition of Zn catalysts at various Zn precursor concentrations.	21
Figure 6. Schematic of the CO ₂ ER in KHCO ₃ aqueous solution.	23
Figure 7. Schematic of the CO ₂ ER in IL.	23
Figure 8. SEM images of (a) 0.05Zn/Cu and (b) 0.05Zn/Ti.	29
Figure 9. XRD patterns of (a) 0.05Zn/Cu and (b) 0.05Zn/Ti.	30
Figure 10. SEM images of (a) Zn foil, (b) Cu foil, (c) 0.025Zn/Cu, (d) 0.05Zn/Cu, (e) 0.1Zn/Cu, (f) 0.2Zn/Cu, and (g) 0.4Zn/Cu.	36
Figure 11. XRD patterns of (a) Zn foil, (b) Cu foil, (c) 0.025Zn/Cu, (d) 0.05Zn/Cu, (e) 0.1Zn/Cu, (f) 0.2Zn/Cu, and (g) 0.4Zn/Cu.	39
Figure 12. LSV curves of 0.05Zn/Cu in N ₂ and CO ₂ saturated solutions (0.1M KHCO ₃ and IL) with a scan rate 100 mV/s.	42
Figure 13. SEM images of (a) 0.05Zn/Cu in 0.1M KHCO ₃ and (b) 0.05Zn/Cu in IL after run reaction.	44

CHAPTER I

INTRODUCTION

1.1 Introduction

Nowadays, the amount of carbon dioxide (CO₂) in the atmosphere is rising because the depletion of fossil fuels has increased, made by global population growth and economic advancement [1, 2] This phenomenon has resulted in global climate problems such as the greenhouse effect, thus the sustainable technologies to decline the impact of pollution are grown.

Different methods have been employed to convert CO₂ into fuels for example, thermochemical, electrochemical, and photochemical methods [3-7]. Among these technologies, the electrochemical carbon dioxide reduction (CO₂ER) is an attractive technique because of its feature compared with other methods. Firstly, the reaction can be carried out at ambient conditions. Secondly, the operating reaction parameters (e.g., metal, electrolyte, and redox potential) can be modified to obtain various products. Thirdly, the CO₂ER can entirely utilize renewable energy as power sources [8-10].

The CO₂ER products contain carbon monoxide (CO), methane (CH₄), methanol (CH₃OH), formate (HCOOH), ethylene (C₂H₄), and ethanol (C₂H₅OH), etc.[1] Considering all CO₂ER products, CO is an essential product because it is mainly used as a feedstock for the Fischer–Tropsch synthesis, methanol production, and pharmaceutical industry. It is also easy to be extracted from electrolytes [11, 12]. However, the CO₂ molecules are difficult to be reduced because the CO₂ER requires a high reduction potential to activate the reduction process [13, 14]. Therefore, to improve this process, many researchers aim to study electrocatalysts and electrolyte.

For CO production, the most selective catalysts are Au, Ag, and Zn. Among these catalysts, Zn is an encouraging catalyst because it is low-priced, available, low-toxic, and proper to further scale up for industrial applications [15-18]. Generally, the Zn electro-catalyst is built by various methods such as electrodeposition [19, 20] and paste drying [21]. Many exhaustive studies describe the electrodeposition as a distinguishing process. Due to effective controlling the shape of the metal deposited, it is simple to operate at room temperature [22, 23]. Accordingly, Zn electrodeposition

was applied under various operating conditions to optimize the performance of the Zn electrocatalyst.

While the electrocatalysts are indispensable in the catalytic reaction, the electrolyte used as a medium for the reduction process plays a crucial role in reducing reaction. Recently, there are several electrolytes, such as aqueous electrolytes, organic electrolytes, and ionic liquids (ILs), that are employed in the CO₂ electrochemical reduction [24, 25].

Among them, ILs are attractive electrolytes, consisting of large organic cations and small inorganic anions [26]. Their outstanding traits show strong absorption for CO₂ [27, 28], high electrical conductivity, and high stability [29-32]. Thus, the CO₂ER in ILs-based electrolytes is imperative to magnify the electrochemical performance.

In this work, the Zn electrocatalysts were prepared by Zn electrodeposition on different substrates (copper (Cu) and titanium (Ti) foil). The better substrate was selected to further study the effect of Zn precursor concentration. Then, the catalysts were tested in the CO₂ER in an aqueous electrolyte. The morphology, bulk composition, and crystalline structure of these catalysts were identified by various characterization such as scanning electron microscope-energy dispersive X-ray spectroscopy (SEM-EDX) and X-ray diffraction (XRD). Finally, the catalyst that exhibited the best performance in terms of the highest CO production in the aqueous electrolyte, was evaluated in CO₂ER in ILs to compare the activity CO₂ER between the two systems.

1.2 Objectives of the Research

1. To study the characteristics and the CO₂ER performances of Zn electrocatalysts prepared by Zn electrodeposition on different substrates (Cu, Ti).
2. To investigate the effects of Zn precursor concentration, by using the better substrate from the first objective, on the characteristics and the activity in the CO₂ER.
3. To analyze the CO₂ER activity between the reaction passing in aqueous electrolyte and ionic liquid (IL) with the best Zn electrocatalyst.

1.3 Scopes of the Research

1. Before the electrodeposition and electrolysis experiments, Zn foil ($10 \times 25 \text{ mm}^2$) Cu foil ($10 \times 25 \text{ mm}^2$), and Ti foil ($10 \times 25 \text{ mm}^2$) were mechanically polished with 800G sandpaper and were rinsed with DI water before, then left to dry at room temperature.

2. The substrates used in this study were Cu and Ti foils.

3. The Zn electrocatalysts were prepared by electrodeposition of Zn on the best substrate (Cu or Ti) at different precursor concentrations of Zn that changing from 0.025 M to 0.4 M. The current density for electrodeposition was set at 20 mA/cm^2 . Pt rod was used as counter electrode. After the electrodeposition method, the catalysts were cleaned with deionized water several times before leaving them to dry at room temperature.

4. 20 mL of KHCO_3 0.1 M was used as aqueous solution for both catholyte and anolyte. Before the electrolysis experiment, electrolyte was saturated with 100 mL/min CO_2 gas for 30 minutes. While the CO_2ER was carried out by using 20 mL/min CO_2 flow rate.

5. ILs used in this study is the mixture of propylene carbonate (PC), 1-butyl-3-methylimidazolium tetrafluoroborate ($[\text{BMIM}]\text{BF}_4$), and water at 5:4:1 volume ratio, respectively.

6. A potentiostat (Metrohm Autolab) was used for the electrodeposition method and the CO_2ER experiments.

7. The catalysts were characterized by

1. Scanning electron microscope-energy dispersive X-ray spectroscopy (SEM-EDX)

2. X-ray diffraction (XRD)

CHAPTER II

BACKGROUND AND LITERATURE REVIEWS

2.1 Fundamental of electrochemical reduction of CO₂

Table 1 concludes the equilibrium potentials used in term the standard hydrogen electrode (SHE) at pH 7.0 aqueous solution for different products [33]. Although the formation of methane (CH₄) and ethylene (C₂H₄) can be made at lower negative potentials than that of the hydrogen evolution reaction (HER), the kinetic energy of the CO₂ER is still high. This is caused from the step of CO₂ to form CO₂ anion radical (CO₂^{•-}). This step requires -1.9 V by without catalysts for rearrangement of CO₂ molecule from a straight form into a bend anion radical [34, 35]. Usually, the formation of this intermediate step is called the rate determining step [36]. As a result, the actual potentials that applied to produce products are more negative than equilibrium potentials. Thus, the appearance of electrocatalysts for the CO₂ER decreases the kinetic energy barriers and boosts the energy efficiency.

Table 1. Standard electrochemical potentials for CO₂ reduction.

Reduction potentials of CO ₂	E° [V] vs SHE at pH 7
$\text{CO}_2 + \text{e}^- \rightarrow \text{CO}_2^{\bullet-}$	-1.9
$\text{CO}_2 + 2\text{H}^+ + 2\text{e}^- \rightarrow \text{HCOOH}$	-0.61
$\text{CO}_2 + 2\text{H}^+ + 2\text{e}^- \rightarrow \text{CO} + \text{H}_2\text{O}$	-0.52
$2\text{CO}_2 + 12\text{H}^+ + 12\text{e}^- \rightarrow \text{C}_2\text{H}_4 + 4\text{H}_2\text{O}$	-0.34
$\text{CO}_2 + 4\text{H}^+ + 4\text{e}^- \rightarrow \text{HCHO} + \text{H}_2\text{O}$	-0.51
$\text{CO}_2 + 6\text{H}^+ + 6\text{e}^- \rightarrow \text{CH}_3\text{OH} + \text{H}_2\text{O}$	-0.38
$\text{CO}_2 + 8\text{H}^+ + 8\text{e}^- \rightarrow \text{CH}_4 + 2\text{H}_2\text{O}$	-0.24
$2\text{H}^+ + 2\text{e}^- \rightarrow \text{H}_2$	-0.42

2.2 Study on electrodes

Since 1989, metals have been widely explored for CO₂ER electrocatalysts. Hori et al. showed that CO, formate, and other hydrocarbons occurred from the CO₂ER on the surface of metals [37]. The selectivity of products was proven based on the adsorption energy of CO intermediate using density functional theory (DFT) calculations [38]. The reduction of products is used to categorize metals into three groups. The first group includes Sn, Pb, Bi, In, Hg, and Cd. The CO₂ intermediate is difficultly adsorbed on these substrates. Then, the molecule desorbs and changes form to formate or formic acid via protonation. The second group, including Au, Ag, Zn, Pd and Ga, bind on the CO₂ intermediate easily. This intermediate is further reduced to CO because of the weak adsorption energy of the CO intermediate. The third group includes Pt, Ti, Ni and Fe. They are selective for the HER because these metals were inert catalysts with CO intermediate. Thus, they are not competing with CO₂ reduction. Besides three groups, Cu is the only metal used to produce C₁-C₃ hydrocarbons or alcohols passing COH or CHO intermediates [39].

Pathways for CO₂ER have two main routes as shown in Figure 1. The first routes, when CO₂^{•-} is occurring, it will be reacted with water to form HCOO[•] which can be reduced to formate (HCOO⁻). This pathway is relative to the first group as mentioned above. The second route, CO₂^{•-} is protonated from water to form [•]COOH. This intermediate is suddenly reduced to CO. This pathway can be occurred in the second group. Moreover, the CO intermediate on Cu can be reduce to hydrocarbons.

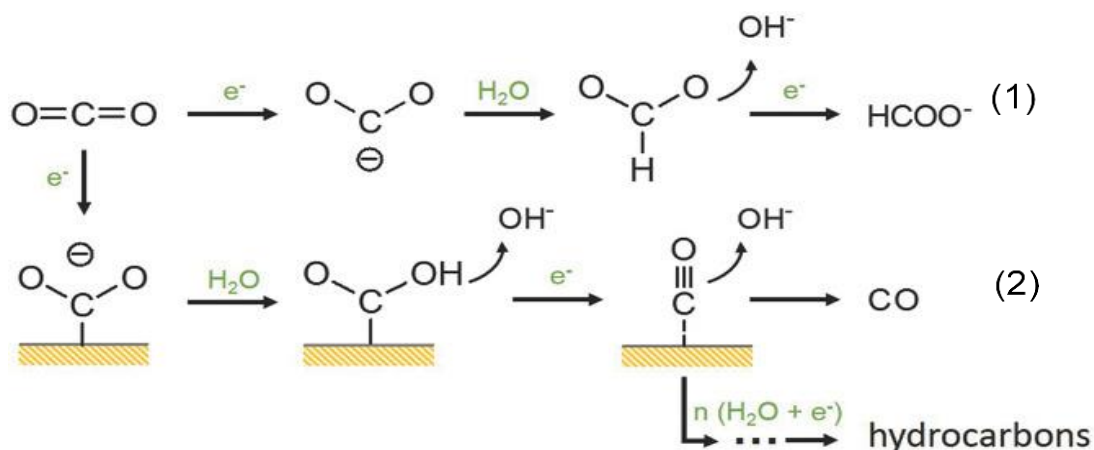


Figure 1. Possible pathways for CO₂ER on metal surfaces in aqueous solution [40].

Table 2-6 show summary of Sn, Au, Zn and Cu electrodes. Faradaic efficiency (FE) is the selectivity of products [41].

Table 2. Sn-based electrode in the CO₂ER.

Electrode	Potential (V)	Faradaic efficiency			Reference
		CO	Formate	Hydrogen	
Sn foil	-1.7 (vs. SCE)	N/A	95%	N/A	Wu, J. 2012 [42]
Sn plate	-1.85 (vs. SCE)	N/A	>91%	N/A	Lv, W. 2014 [43]
Sn quantum sheets/GO	-1.8 (vs. SCE)	N/A	89%	~2%	Lei, F. 2016 [44]
Sn _{56.3} Pb _{43.7} /carbon paper	-2 (vs. Ag/AgCl)	N/A	~79.8%	~18.7%	Choi, S.Y. 2016 [45]
AgSn/SnO _x	-0.8 (vs. RHE)	N/A	~80%	N/A	Jiao et al. 2017 [46]
Urchin-like SnO ₂	-1.0 (vs. SHE)	N/A	62%	N/A	Liu, Y. 2017 [47]
Sn-CF1000	-0.8 (vs. RHE)	23%	65%	12%	Zhao, Y. 2018 [48]
Sn rod/graphite	-1.65 (vs. Ag/AgCl)	N/A	94.5%	N/A	Yadav, V. S. K. 2018 [49]
SnO _x /AgO _x	-0.8 (vs. RHE)	N/A	>95%	<5%	Choi, Y.W. 2019 [50]
Sn foam	-1.6 (vs. Ag/AgCl)	N/A	95.6	N/A	Li, D. 2019 [51]
Sn-Polyaniline/Ni foam	-1.7 (vs. Ag/AgCl)	N/A	~94%	N/A	Li, F. 2020 [52]
SnO ₂ /CF-40	-1.0 (vs. RHE)	N/A	86%	N/A	Li, H. 2020 [53]
Sn _{0.80} Bi _{0.20} @ Bi-SnO _x	-1.38 (vs. RHE)	N/A	95.8%	N/A	Yang, Q. 2020 [54]
Nanorod@sheet SnO	-0.7 (vs. RHE)	N/A	94%	N/A	Qian, Y. 2020 [55]
Sn/Nano-Cu	-1.2 (vs. RHE)	N/A	86.80%	N/A	Chen, G. 2021 [56]
OCSn/CP	-1.13 (vs. RHE)	N/A	92%	N/A	Zhong, H. 2021 [57]

Table 3. Au-based electrode in the CO₂ER.

Electrode	Potential (V)	Faradaic efficiency			Reference
		CO	Formate	Hydrogen	
Planar polycrystalline Au	-0.4(vs. RHE)	50%	N/A	N/A	Chen, Y. 2012 [58]
oxidized-derived Au	-0.4 (vs. RHE)	~98%	~1%	N/A	Chen, Y. 2012 [58]
2.7 μ m Au-IO	-0.4 (vs. RHE)	75%	N/A	20%	Hall, A.S. 2015 [59]
PF-Au-75	-0.5 (vs. RHE)	90.5%	N/A	N/A	Chen, C. 2017 [60]
PF-AuAg-75	-0.5 (vs. RHE)	88%	N/A	N/A	Chen, C. 2017 [60]
Au foil	-1.0 (vs. RHE)	~30%	N/A	N/A	Andrews, E. 2018 [61]
Bulk Cu ₇₅ Au ₂₅	-1.0 (vs. RHE)	~45%	N/A	N/A	Andrews, E. 2018 [61]
NPS 2 nm Cu ₂₅ Au ₇₅	-0.75 (vs. RHE)	~35%	N/A	N/A	Andrews, E. 2018 [61]
NPS 6 nm Cu ₉ Au ₉₁	-0.95 (vs. RHE)	~70%	N/A	N/A	Andrews, E. 2018 [61]
Au/PANI	-0.7 (vs. RHE)	90.3%	N/A	N/A	Yu, J. 2021 [62]
NPAuCu	-0.4 (vs. RHE)	73.2%	N/A	N/A	Liu, Z. 2021 [63]

Table 4. Ag-based electrode in the CO₂ER.

Electrode	Potential (V)	Faradaic efficiency			Reference
		CO	Formate	Hydrogen	
Ag ₅₇ Cu ₄₃	-1.7 (vs. SCE)	~10%	N/A	~70%	Choi, J. 2016 [64]
Ag ₁₀₀ /Cu foil	-1.7 (vs. SCE)	64.6%	N/A	~10%	Choi, J. 2016 [64]
Ag/Cu foil	-1.5 (vs. SCE)	37.2%	N/A	~43%	Park, H. 2017 [65]
Ag foil	-1.5 (vs. SCE)	30.2%	N/A	~12%	Park, H. 2017 [65]
Ag _{85.4} In _{14.6}	-1.5 (vs. SCE)	75.5%	N/A	~20%	Park, H. 2017 [65]
Ag foam	-1.12 (vs. RHE)	82.9%	~2%	~20%	Yu, Y. 2019 [66]
Pristine Ag	-1.12 (vs. RHE)	79%	~3%	~20%	Yu, Y. 2019 [66]
Nanoporous silver	-0.36 (vs. SCE)	96%	N/A	N/A	Qian, Y. 2020 [67]
Ag/C	-0.82 (vs. SCE)	95.1%	N/A	~5%	Yun, H. 2021 [68]

Table 5. Zn-based electrode in the CO₂ER.

Electrode	Potential (V)	Faradaic efficiency			Reference
		CO	Formate	Hydrogen	
Zn-MOF ^{NO3}	-1.8 (vs. SCE)	69.8%	N/A	~29%	Wang, Y. 2017 [69]
Multilayered Zn nanosheets	-1.13 (vs. RHE)	86%	N/A	~15%	Zhang, T. 2018 [70]
Zn foil	-1.13 (vs. RHE)	10%	N/A	90%	Zhang, T. 2018 [70]
Porous network Zinc	-1.77 (vs. SCE)	~80%	~10%	~10%	Lu, Y. 2018 [1]
Porous Zn	-0.95 (vs. RHE)	94.4%	N/A	N/A	Luo, W. 2019 [71]
ZnO-3	-0.85 (vs. RHE)	90%	N/A	<5%	Luo, W. 2020 [72]

Table 6. Cu-based electrode in the CO₂ER.

Electrode	Copper foil	Cu oxide NNS
Potential (V)	-1.69 (vs. SCE)	-1.84 (vs. SCE)
Faradaic efficiency	CO	N/A
	Formate	~19%
	Hydrogen	~17%
	Methane	~14%
	Ethylene	~6%
	Ethanol	N/A
	n-Propanol	N/A
	Allyl alcohol	N/A
References	Kuhl, K .P. 2012 [39]	Xie, J. 2015 [73]

2.3 Electrodeposition of Zn electrocatalysts.

Electrodeposition or electroplating is a method that is applied for coating a metal onto a substrate via the electrochemical reduction of metal ions. The electroplating system consists of the object that needs to be covered, called a cathode, electrolyte, an anode, and a power source. The primary function of electrolyte is conductivity which some electrolyte has low conductivity. Adding supporting electrolytes, such as salt, inorganic acids, and alkali can improve this problem. Significantly, these substances can also decrease the potential input [74].

The overall reaction of the electrolysis is illustrated in the following equations. Eq. 1, Eq. 2, and Eq. 3 are reduction reaction, oxidation reaction for the soluble anode, and oxidation reaction for the inert anode.



Figure 2 represents the mechanism of the cathodic deposition. In the first step, the change from metal ions in bulk solution to hydrated ions form ($M(H_2O)_x^{z+}$), where x is the number of water molecules surrounding metal ions, is happened. While these molecules are being transported to the cathode surface, water molecules arrange in a parallel plane in the diffusion layer. Then, these water molecules are detached from hydrated ions in the Helmholtz layer. In the next step, metal ions move towards the cathode surface and are adsorbed by the electron source's electrostatic force. At the cathode surface, atoms' growth is occurred, which can grow into the crystal lattice [75].

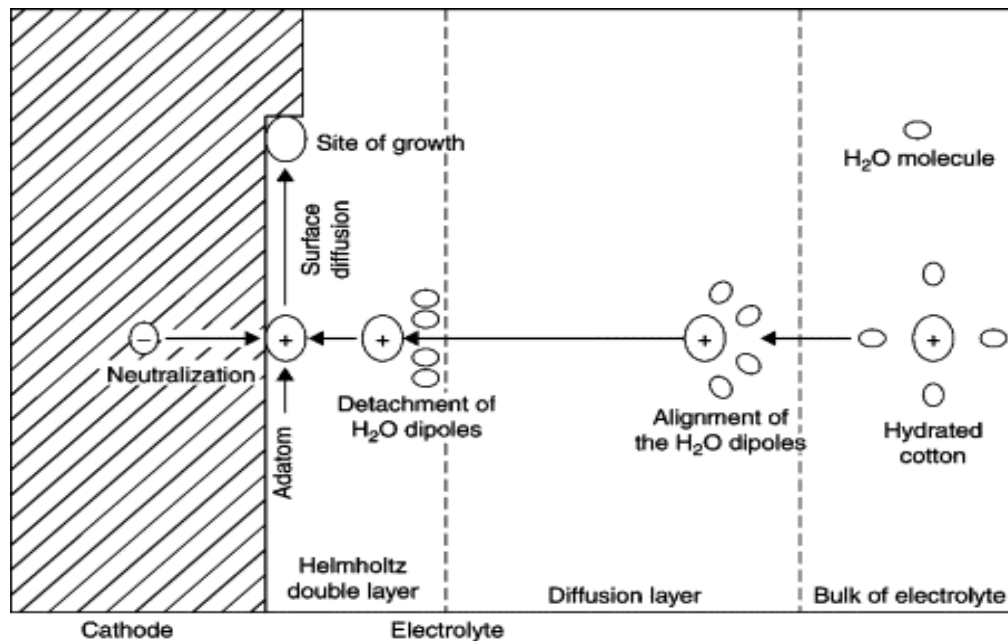


Figure 2. Diagram of steps in the cathodic deposition of metals.

The amount of metal deposited (W) on the cathode surface is calculated from the electrochemical equivalent of the metal (z_c) and the product of the amount of total coulombs passed (Q_c).

$$Q_c = \int I dt \quad (4)$$

$$z_c = M_w / nF \quad (5)$$

$$W = \int I dt M_w / nF \quad (6)$$

Where I is applied current, t is a period, M_w is metal's molecular, F is faradaic constant and n is number of electron [75].

Table 7. Zn electrocatalysts by electrodeposition method.

Researcher	Electrode name	Catalyst preparation	Faradaic efficiency
Alias, N. et al. (2015) [76]	Zn/Cu	A Cu plate ($1 \times 5 \text{ cm}^2$) was used as the substrate and a Zn plate ($2 \times 4 \text{ cm}^2$) was used as the anode for electrodeposition process. Their surfaces were polished using a common metallographic technique. Then, these electrodes were sonicated in acetone for 10 min and were rinsed with deionized water. Zn was electrodeposited, passing a solution of 1 M ZnSO_4 for 1 hr. Area of the Cu plate for deposition was fixed at 1 cm^2 and the applied currents were varied in different values (0.01, 0.02, 0.04, 0.08, and 0.1 A cm^{-2}).	-
Luo, Wu. et al. (2019) [71]	Porous Zn (P-Zn)	P-Zn was electrodeposited on a Cu mesh in the electroplating bath, containing 1.5 M $(\text{NH}_4)_2\text{SO}_4$ and 0.1M $\text{ZnSO}_4 \cdot 7\text{H}_2\text{O}$. The electrodeposition was operated at a constant current density of -1.0 mA/cm^2 for 30 s.	CO : 95% at -0.95 V vs. RHE
	Zn foil	A Zn electrode was mechanically polished using sandpaper. Then, this foil was sonicated in water. In electrodeposited process,	CO : 50% at -0.95 V vs. RHE
	Porous Zn -based gas diffusion electrode (P-Zn-based GDEs)	Zn was deposited on a Cu mesh using the same solution of P-Zn at -0.25 mA cm^{-2} for 60 s. Then, this sample was washed and dried before the electrode was immersed into PTFE solution. Next step, PTFE mixed with carbon black dispersion in ratio 1 to 1 was coated on the sample to form a hydrophobic layer. Finally, the sample was conducted in heater at $350 \text{ }^\circ\text{C}$ in N_2 for 30 min	CO : 84% at -0.64 V vs. RHE

Researcher	Electrode name	Catalyst preparation	Faradaic efficiency
Lu, Y. et al. (2018) [1]	ED Zn	ED Zn was fabricated by electrodeposition of Zn on Zn foil (0.5 cm×2.5 cm) in 0.05M Zn(NO ₃) ₂ . Multi-step potentials were used in electrodeposited method to study the effects of cycles and applied potentials. The applied potential was conducted to -1 V for 3 s. Then, potential of -1 V was increased to -2.5 V (vs. Ag/AgCl) for 3 s and these steps were repeated 90 times. The prepared catalyst was cleaned with deionized water and ethanol and suddenly introduced for the CO ₂ ER to avoid oxidation of electrode.	CO : 80% at -1.1 V vs. RHE
	ED Zn-2	According to the synthesized ED Zn, the solution for electrodeposition method was used same as mentioned above. ED Zn-2 was prepared by using multi-step potentials for 0.3 s in each potential of -2 V and -2.5 V (vs. Ag/AgCl) and these steps were repeated 90 times.	CO : 70% at -1.1 V vs. RHE
	ED Zn-3	ED Zn-3 was prepared by using multi-step potentials for 6 s in in each potential of -2 V and -2.5 V (vs. Ag/AgCl) and these steps were repeated 30 times.	CO : 60% at -1.1 V vs. RHE
Luo, W. et al. (2020) [72]	Zinc oxide (ZnO)	Zn (1cm×0.5cm) foil was cleaned with 2 M HNO ₃ , acetone and deionize water, respectively before it was used as a substrate. ZnO was synthesized by the electrodeposition of Zn on Zn foil in 0.01 M Zn(NO ₃) ₂ and 0.1 M KCl at 60 °C for 2 h. The current density was fixed at -4 mA cm ⁻² for electrodeposited method. The obtained ZnO was reduced to Zn at -1.6 V (vs. RHE) in CO ₂ saturated 0.1 M KHCO ₃ for 20 min.	CO: ~90% H ₂ : ~10% at -0.85 V vs. RHE

Researcher	Electrode name	Catalyst preparation	Faradaic efficiency
	Zn-B, Zn-D	The precursor for electrodeposition method contained 0.05 M ZnCl ₂ at -20 mA cm ⁻² for 3 min, which this catalyst was labeled Zn-B. The another catalyst was deposited in 0.1M ZnSO ₄ and 1.5 M (NH ₄)SO ₄ at -500mA cm ⁻² for 20 s, which this sample was labeled Zn-D.	CO :~45% for Zn-B, CO :~70% for Zn-D at -0.7 V vs. RHE
Rosen, J. et al. (2015) [17]	Zn dendrites	Zn foil were polished using sand paper. Then, this substrate was sonicated in acetone and water. Zn dendrite electrode was prepared by electrodeposition of Zn on Zn foil in ZnO mixed with 6 M KOH. The experiment was set at -1.0 A cm ⁻² for 60 s. After deposition was finished, the electrode was rinsed with deionized water and used to test in CO ₂ ER.	CO : 79 % at -1.1 V vs. RHE

Alias, N. et al. (2015) [76] studied the morphology of Zn in different forms, which got from electrodeposition of Zn on Cu at various current densities (0.02, 0.04, 0.08, and 0.1 A/cm²), to apply as anode for Zn-batteries. The results showed a low current density (0.01 A/cm²) provided a thin layer of Zn on Cu. When the current density was increased to 0.02 A cm⁻², the morphology transformed into a hexagonal structure. At high current densities (> 0.04 A/cm²), Zn's structure changed to a flake-like form. This paper indicated that the rate of deposition was proportional to the increasing of current density. However, a very high current density affected the structure's change from high dense to dendritic, which this shape was not stable. Thus, a current density of 0.02 A/cm² was chosen as the best condition. Besides, it was observed that the dominant peak of Zn at (101) plane, which was corresponded to pure Zn at the optimum current density

Luo, Wu et al. (2019) [71] studied different catalysts' performance, which included P-Zn, Zn foil, and P-Zn-based GDEs. The results showed that the P-Zn got higher current density and CO selectivity than those obtained from Zn foil because of the higher surface area. The Cu mesh used as support played the primary role in increasing

the surface area of P-Zn. Because this substrate had high conductivity, the uniform Zn particles were deposited on the surface. At -0.95 V (vs. RHE), the P-Zn exhibited a higher catalytic activity, such as CO FE of 95 % and current density of 27 mA/cm², compared with that of Zn foil (CO FE = 50 %, current density < 5 mA/cm²). However, the study of kinetic showed the low intrinsic activity of two catalysts. Thus, P-Zn-based GDEs were applied in a flow reactor to improve this property, which was believed that this affected by the mass transfer effect. A flow cell, in which the gas and liquid phases were separated by a gas diffusion electrode (GDE) to decrease mass-transfer limitations, showed the highest FE for CO (84%) and current density (200 mA/cm²) at -0.64 V.

Lu, Y. et al. (2018) [1] studies the different morphologies of the Zn catalysts influencing the catalytic activity by varying the electrodeposition conditions. The results presented the three catalysts (ED Zn, ED Zn-2, ED Zn-3) had the appearance of a porous form, which contained a number of particles. As the various electrodeposition conditions, they affected the different particle size of these catalysts. The ED Zn exhibited a smaller particle size than that the other electrodes, which resulted in a lot of surface area. Moreover, when the particles were small, the low-coordinated surface sites will be dominant. As a higher active surface area, the CO FE of ED Zn (80 %) was higher than that of the other catalysts (FE 70% for ED Zn-2 and FE 60% for ED Zn-3) at -1.1 V (vs. RHE). Hence, the porous Zn catalyst, which consisted of the smallest nanoparticles (size 30 nm), provided the highest CO₂ER activity.

Luo, W. et al. (2020) [72] studies the three ZnO catalysts obtained from various preparation methods, containing hydrothermal, spray-coating, and electrodeposition method. The results showed that the ZnO catalysts' morphologies appeared in the form of nanowires, nanoparticles, and nanoflowers. Then, the obtained ZnO samples were reduced at -1.6 V (RHE) to generate metallic Zn. As the metallic Zn increased, all these catalysts changed from previous forms to thin hexagonal flakes, which exhibited a higher surface area. This morphology was occurred by reconstruction of the structure of Zn, in which ZnO dissolved in ions form, and then these molecules grow into Zn crystals. It was concluded that the occurring hexagonal structure was independent of their initial morphologies. When these catalysts were experimented with in CO₂ER,

increasing the surface area of ZnO enhanced the CO FE and the current densities in the studied potential compared to those of the bulk Zn catalysts.

This literature also studied the effects of various electrodeposition conditions, including ZnNO₃, ZnCl₂, and ZnSO₄ used as a precursor for the electrodeposition method. The results indicated that the different precursors affected the morphologies catalysts. In the ZnNO₃ solution, the morphology showed a nanoflower form, which will be changed in thin hexagonal flakes after reducing these catalysts as mentioned above. In the ZnCl₂ and ZnSO₄ solution, the morphology showed a nanoflower mixed with hexagonal form and dendritic form. It was found that the performance of these catalysts was based on the electrochemical surface active area (ESCA) and the local pH. During CO₂ER, the local pH (>8) values were higher than the bulk pH (6.8). This showed that the increased local pH was caused by consuming proton of both CO₂ER and HER. Thus, the local pH was proportional to the current density and the surface area of catalysts.

Rosen, J. et al. (2015) [17] studied the electrodeposition conditions by changing the current densities to investigate the obtained morphologies. The results showed that a mossy morphology was found at low deposition rates (~10 mA cm⁻²), which this form was too weak to test in the CO₂ER. As a higher deposition rate in the medium region (~20 mA cm⁻²), the morphology displayed a bulky morphology, which has a low surface area. When the current density was an increase to 1 mA/cm², the Zn dendrites could be formed. In the CO₂ER, the Zn catalyst with dendritic form was used as cathode because it showed the nanostructure, resulting in a higher surface area. The highest CO FE (79%) of a dendritic Zn was achieved at -1.1 V (vs. RHE), which this value was higher than that of the bulk Zn foil (CO FE < 35%). During the running reaction, the Zn catalyst could be redeposited to a substrate with a crystal-like form.

2.4 Ionic liquids (ILs)

Electrolytes are a necessary medium exploited for the CO₂ER. An important duty of electrolytes is delivering electron and proton species to easily occur reactivity. As electrolytes are an important variable, plenty of scientists provide attention for selecting electrolytes to enable product selectivity. Electrolytes are classified into three types

such as aqueous electrolytes, organic electrolytes, and ionic liquids. The advantages and disadvantages of these electrolytes as illustrated in Table 8.

Table 8. Comparison between the advantages and the disadvantages in various solutions [29, 77, 78]

Solutions	Advantages	Disadvantages
Aqueous electrolytes	<ul style="list-style-type: none"> - Low cost - Wide availability - High sustainability 	<ul style="list-style-type: none"> - Low CO₂ solubility - Low conductivity - Promoting HER
Organic electrolytes	<ul style="list-style-type: none"> - High CO₂ solubility - Suppressing HER 	<ul style="list-style-type: none"> - High price - High toxicity
Ionic liquids	<ul style="list-style-type: none"> - High CO₂ solubility - Good solvent stability - Recyclability - Low energy demand - Friendly environment - High conductivity 	<ul style="list-style-type: none"> - High price - High viscosity

From considering the merits and demerits of the three electrolytes, ILs expose the outstanding features rather than other electrolytes. Most ILs have excellent conductivity, high stability in a wide potential range, and strong CO₂ solubility. Additionally, because of low their solubility, they are safe for the environment. Furthermore, ILs have not water content which results in suppressing the HER. Thus, ILs are the leading candidate which are received attention from scientists to further study for the CO₂ER. ILs contain large bulky asymmetric organic cations and small inorganic anions which, these molecules have interacted with Coulomb force [26]. The common structures of cations and anions of ILs are shown in Figure 3. There are many studies in the CO₂ER to search the specific structure of ILs, which can provide high activity. The structure of ILs has a prominent role, which lets them bind with CO₂. After that, CO₂ can adsorb easier on the catalyst's surface and decline the activation energy. Thus, the performance of the CO₂ER in ILs can be-improved.

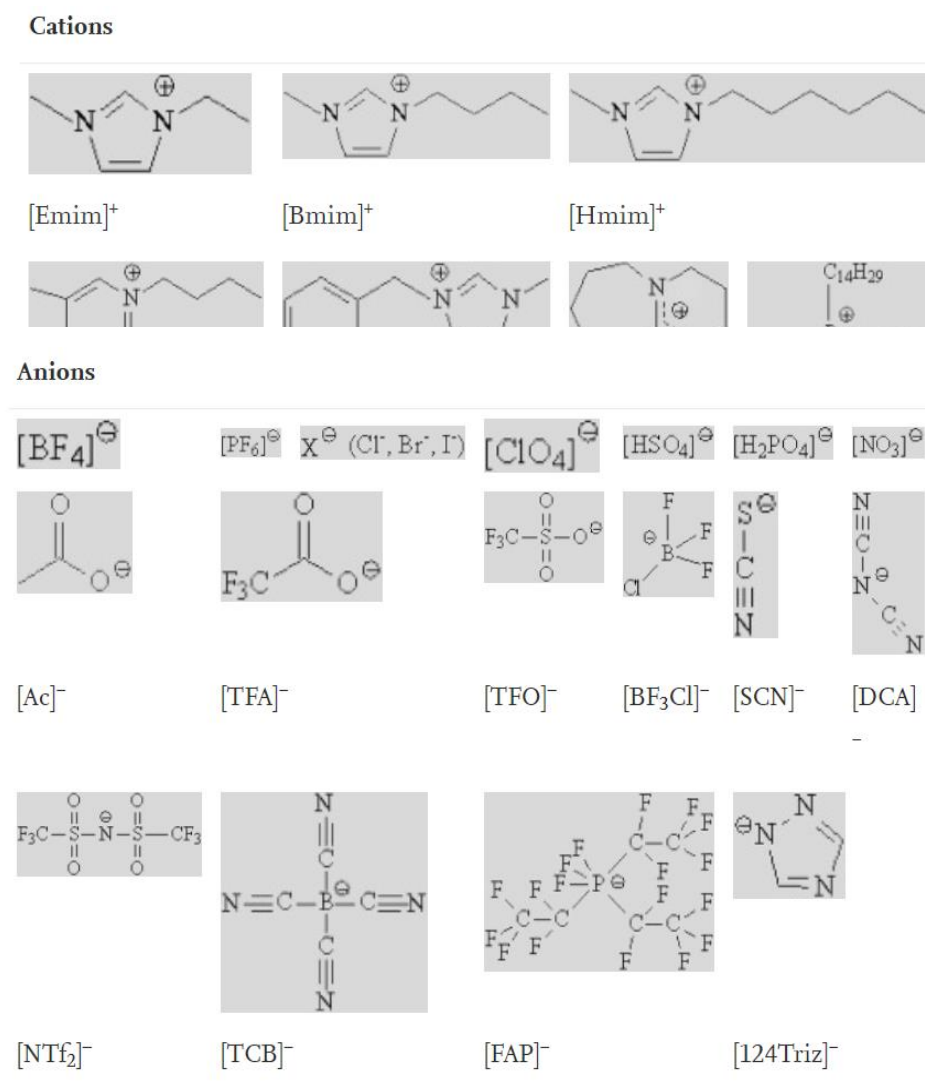


Figure 3. Cations and anions in ILs used the CO₂ER.

Rosen et al. [79] showed that the Addition of 1-ethyl-3-methylimidazolium tetrafluoroborate ([Emim]BF₄) could decrease the overpotential used for CO production on Ag electrode. Liu et al. [80] showed that Ag nanowires occurred reaction in a [EMIm]⁺ based ionic liquid provide 14-times of the current density of CO when compared to that of Ag nanowire in aqueous solution. This thing could be explained that it occurred [EMIm-CO₂]⁺ complexes as intermediates. These molecules would take the CO₂ molecules to surface catalyst, which resulted in good adsorption of CO₂. However, due to a large number of combinations between cations and anions, selecting suit kind of ILs is necessary to enhance the efficiency of the CO₂ER system.

At room temperature, ILs have a high viscosity, decreasing mass transport for exchanging proton and electron. This insufficient property can be improved by mixing some solvents called supporting electrolytes, such as water and organic solvents [81]. Because water is a hindrance in converting CO₂ and can be reduced to H₂ that is an undesired product [82]. Organic solvents are considered instead of water, these organic solvents such as acetonitrile (AN), N,N-dimethylformamide (DMF), and dimethyl sulfoxide (DMSO), which have a limitation for applying in a real situation. AN is not selected as a solvent for ILs because it is a dangerous and volatile substance. In another kind of organic solvent, DMF is also not a suitable solution. It is suffered from hydrolysis in water. For DMSO, at lower room temperature, it is a solid phase which restricts to utilize in some process. Therefore, the finding of appropriate liquid solvents that can be exploited in CO₂ conversion remains a hasty task. So far, propylene carbonate (PC) is a green alternative solvent in electrochemical fields [83]. Because of its low vapor pressure, low-toxic, and natural biodegradable of PC. Moreover, PC also stores a high amount of CO₂, which allows PC to handle the problem faced in CO₂ conversion [84].

For example, in the research that uses PC/ILs as an electrolyte, Ju et al. [85] studied the conversion of CO₂ on an Ag plate in an imidazolium-based electrolyte by varying the alkyl chain length of the imidazolium cations. The results showed that [Bmim]BF₄ was the best ionic liquid because of its low overpotential and high current density compared with other kinds of ILs. The good obtained performance could be explained that the imidazolium cation binded with anion radical (CO₂^{•-}), which occurred stabilizing molecules, which favored in the CO₂ER. Besides, the order of activity of PC/ILs were following [Bmim]BF₄/PC > [Hmim]BF₄/PC > [Emim]BF₄/PC > [Omim]BF₄/PC > [Dmim]BF₄/PC, which the ability adsorption of CO₂ depended on steric hindrance of chain length. Decreasing steric hindrance of chain length caused the higher adsorption of CO₂. However, decreasing from butyl to ethyl cause the thick film layer, which provided a slow diffusion rate of CO₂.

CHAPTER III

MATERIALS AND METHODS

3.1 Materials

Table 9. Chemicals used as precursors and electrolyte.

Chemicals	Formula	Suppliers
Zinc chloride	ZnCl ₂	Sigma-Aldrich
Sodium chloride	NaCl	Emsure
Potassium hydrogen carbonate	KHCO ₃	Acros Organics
1-Butyl-3-methylimidazolium tetrafluoroborate	[BMIM]BF ₄	Sigma-Aldrich
Propylene carbonate	PC	Sigma-Aldrich

Table 10. Metals used as electrodes in electrodeposition method and electrochemical reduction of CO₂.

Electrodes	Suppliers
Copper foil (0.1 mm thick, 99.9999%)	Alfa Aesar
Zinc foil (0.1 mm thick, 99.9999%)	Alfa Aesar
Titanium foil (0.127 mm thick, 99%)	Alfa Aesar
Platinum foil (0.1 mm thick, 99.9999%)	Alfa Aesar
Platinum rod (Length 76 mm, Diameter 2 mm)	Metrohm

3.2 Catalysts preparation

3.2.1 Preparation of electrodes

Zn foil ($10 \times 25 \text{ mm}^2$), Cu foil ($10 \times 25 \text{ mm}^2$), and Ti foil ($10 \times 25 \text{ mm}^2$) as shown in Table 10 were mechanically polished with 800 G sandpaper and were cleaned with DI water. Then, the polished electrodes were dried at room temperature.

3.2.2 Preparation of Zn catalysts

Zn catalysts were deposited on Cu foil ($10 \times 10 \text{ mm}^2$) and Ti foil ($10 \times 10 \text{ mm}^2$) in 0.05 M ZnCl_2 and 0.05 M NaCl, used as a supporting electrolyte, as shown in Table 9 to increase ionic strength solutions via the electrodeposition method. These electrodes were performed in a two-electrode system containing Pt rod used as an anode, and the electrode, which was Cu foil or Ti foil, used a cathode. The current density was fixed at 20 mA/cm^2 for 200 s. during synthesis catalysts. When the electrodeposition process was finished, the Zn catalysts were washed with deionized water before left them dried at room temperature.

Next study, the best substrate was used as a cathode for the fabrication of Zn catalysts. The Zn catalysts were synthesized in a similar manner as mentioned above. The precursors for electroplating bath containing various concentrations of Zn precursor (0.025 M, 0.05 M, 0.1 M, 0.2 M, and 0.4 M) and 0.05 M NaCl were investigated to find the optimum condition. The prepared catalyst were nominated as follows: 0.05Zn/Ti 0.025Zn/Cu, 0.05Zn/Cu, 0.1Zn/Cu, 0.2Zn/Cu, and 0.4Zn/Cu. The obtained catalysts were conducted in an H-type cell to further study in the CO_2ER .

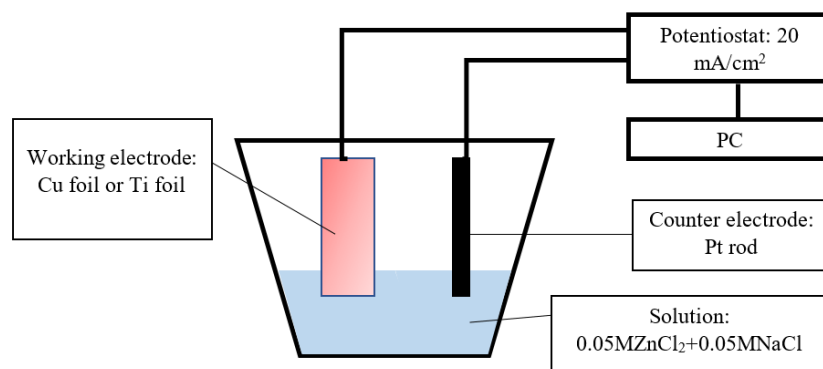


Figure 4. Schematic of electrodeposition of Zn catalysts on different substrates.

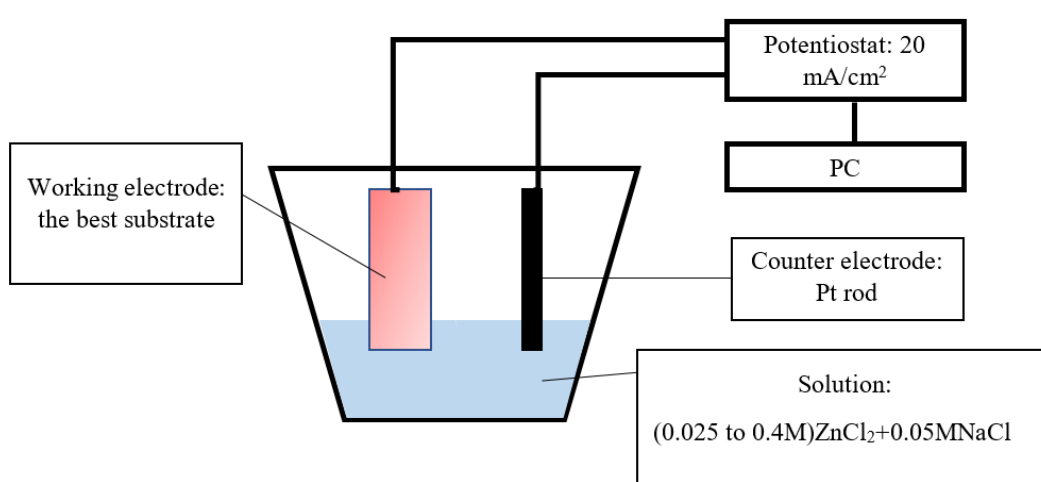


Figure 5. Schematic of electrodeposition of Zn catalysts at various Zn precursor concentrations.

3.3 Catalyst Characterization

3.3.1 Scanning electron microscope-energy dispersive X-ray spectroscopy (SEM-EDX)

Zn foil, Cu foil, 0.05Zn/Ti, 0.025Zn/Cu, 0.05Zn/Cu, 0.1Zn/Cu, 0.2Zn/Cu, and 0.4Zn/Cu were characterized by scanning electron microscopy (SEM) of Hitachi mode S-3400N and energy dispersive X-ray spectroscopy (EDX) to investigate the morphology of the surface and the bulk composition, respectively.

3.3.2 X-ray diffraction (XRD)

The X-ray diffraction (XRD) pattern of electrocatalyst samples were recorded in the 2θ range 20° - 80° (scan rate = 0.5 sec/step) using a Siemens D5000 diffractometer using nickel filtered Cu K_α radiation.

3.4 Electrochemical CO₂ reduction

The CO₂ER was carried out in an H-type cell, and all reaction tests were measured at room temperature and ambient pressure. The cathodic chamber and the anodic chamber were partitioned by Nafion® 117. All the reaction tests were directed in a three-electrode cell consisting of the working electrode, the reference electrode (Ag/AgCl), and the counter electrode (Pt foil). Zn foil, Cu foil, 0.05Zn/Ti, 0.025Zn/Cu, 0.05Zn/Cu, 0.1Zn/Cu, 0.2Zn/Cu, and 0.4Zn/Cu were used as the working electrodes which were put in electrolyte with an area of 1 cm². 20 mL of 0.1 M KHCO₃ was used on both sides of the anode and cathode. The electrolyte was saturated with a CO₂ flow rate of 100 mL/min for 30 minutes. A CO₂ flow rate of 20 mL/min was exploited during the running reaction. A potentiostat tool was used for all the CO₂ER experiments. The potential was fixed at -1.6 V vs. Ag/AgCl. Electrolysis was performed for 70 minutes. The gas chromatography (GC) system with a thermal conductivity detector (TCD) was used to detect H₂ and CO and the operating condition of GC was shown in Table 11. Liquid phase products were analyzed and quantified using NMR. The best Zn electrocatalyst that obtained the highest CO selectivity was further tested in aqueous system as shown in Figure 6 and ionic liquid system as shown in Figure 7.

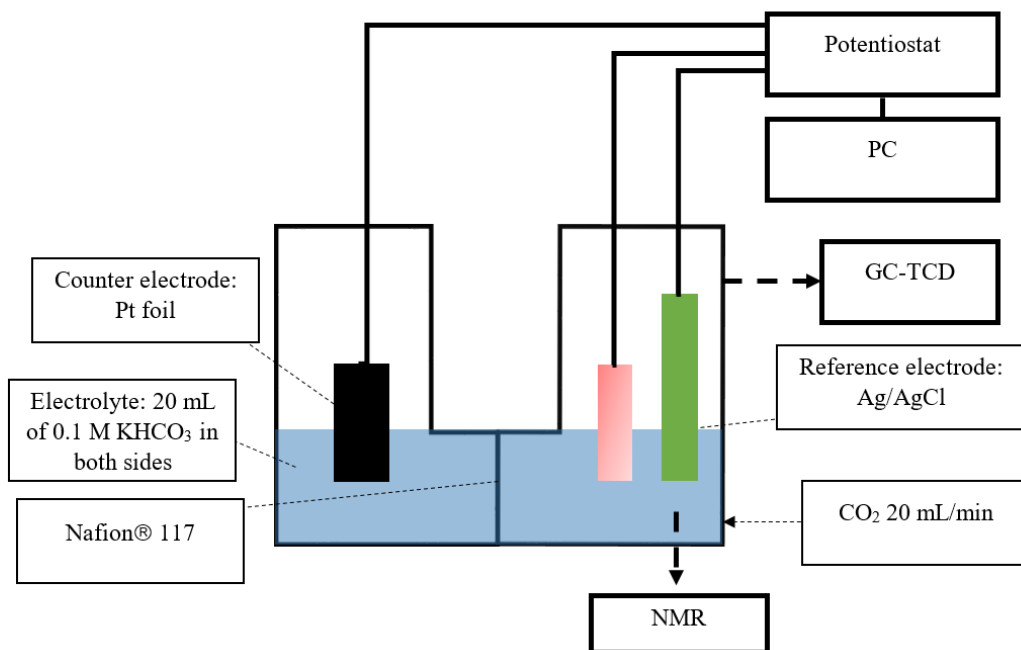


Figure 6. Schematic of the CO₂ER in KHCO₃ aqueous solution.

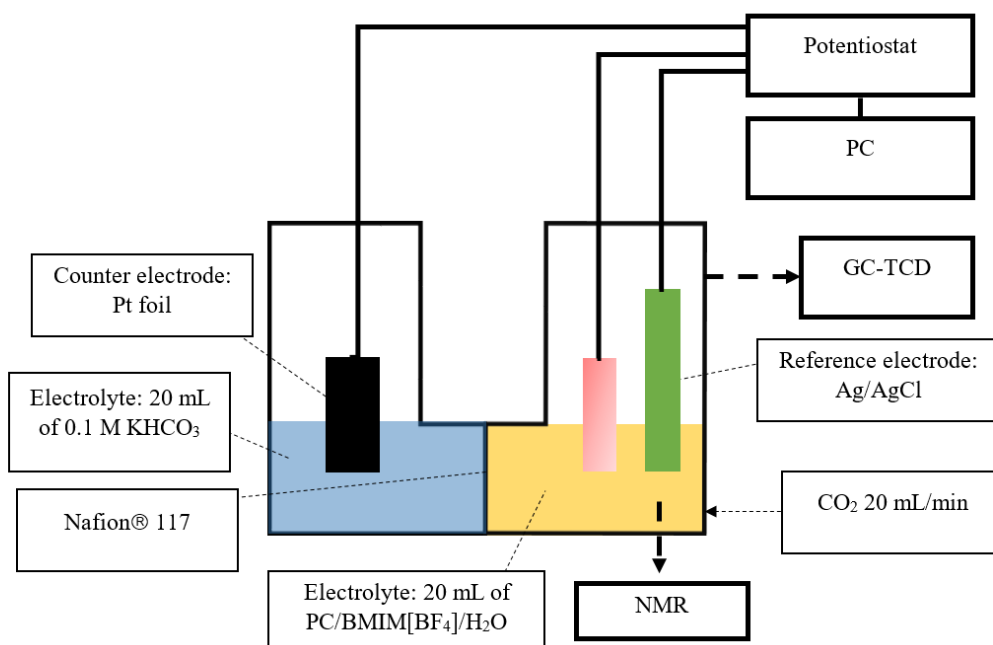


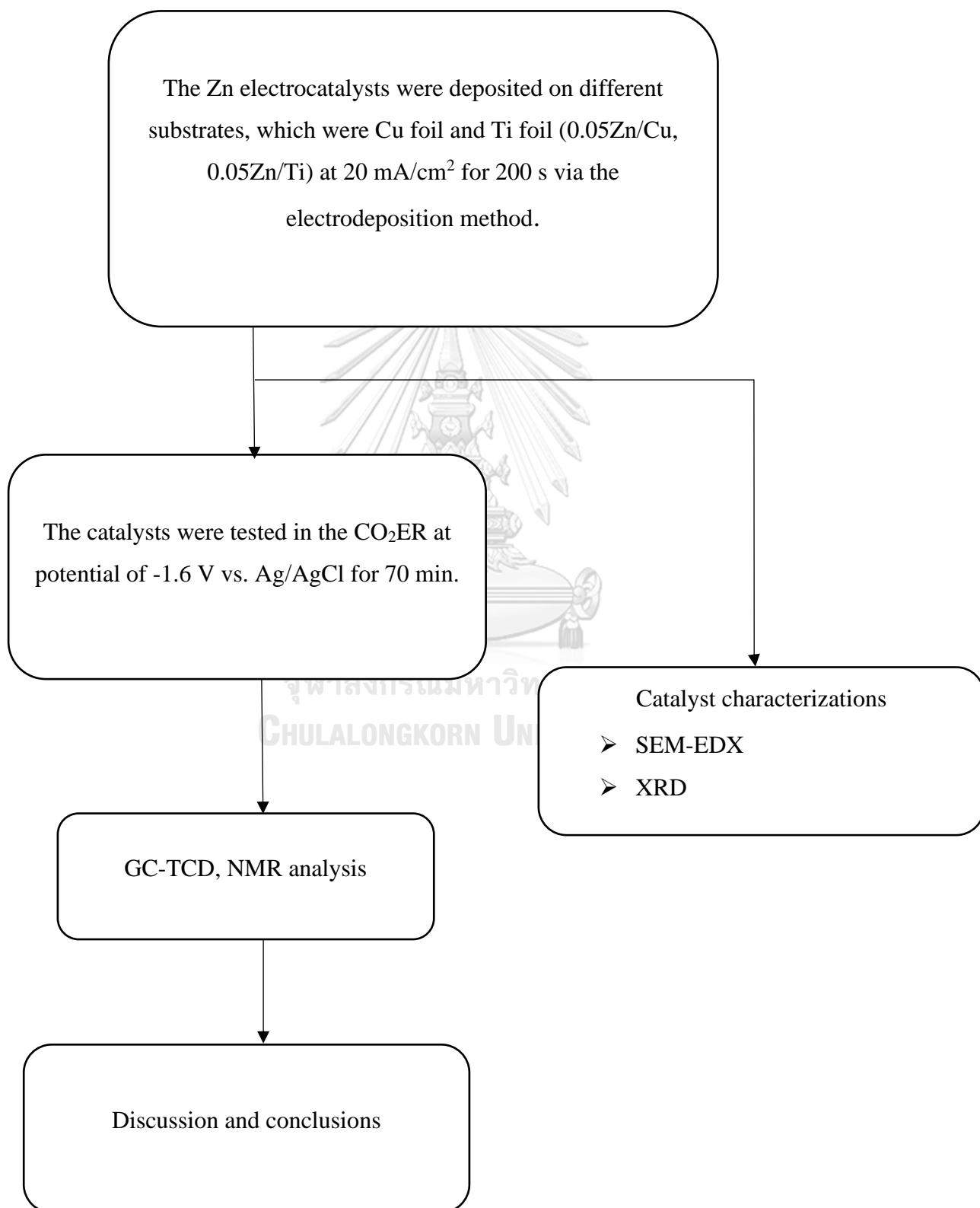
Figure 7. Schematic of the CO₂ER in IL.

Table 11. The operating conditions of gas chromatograph with a thermal conductivity detector.

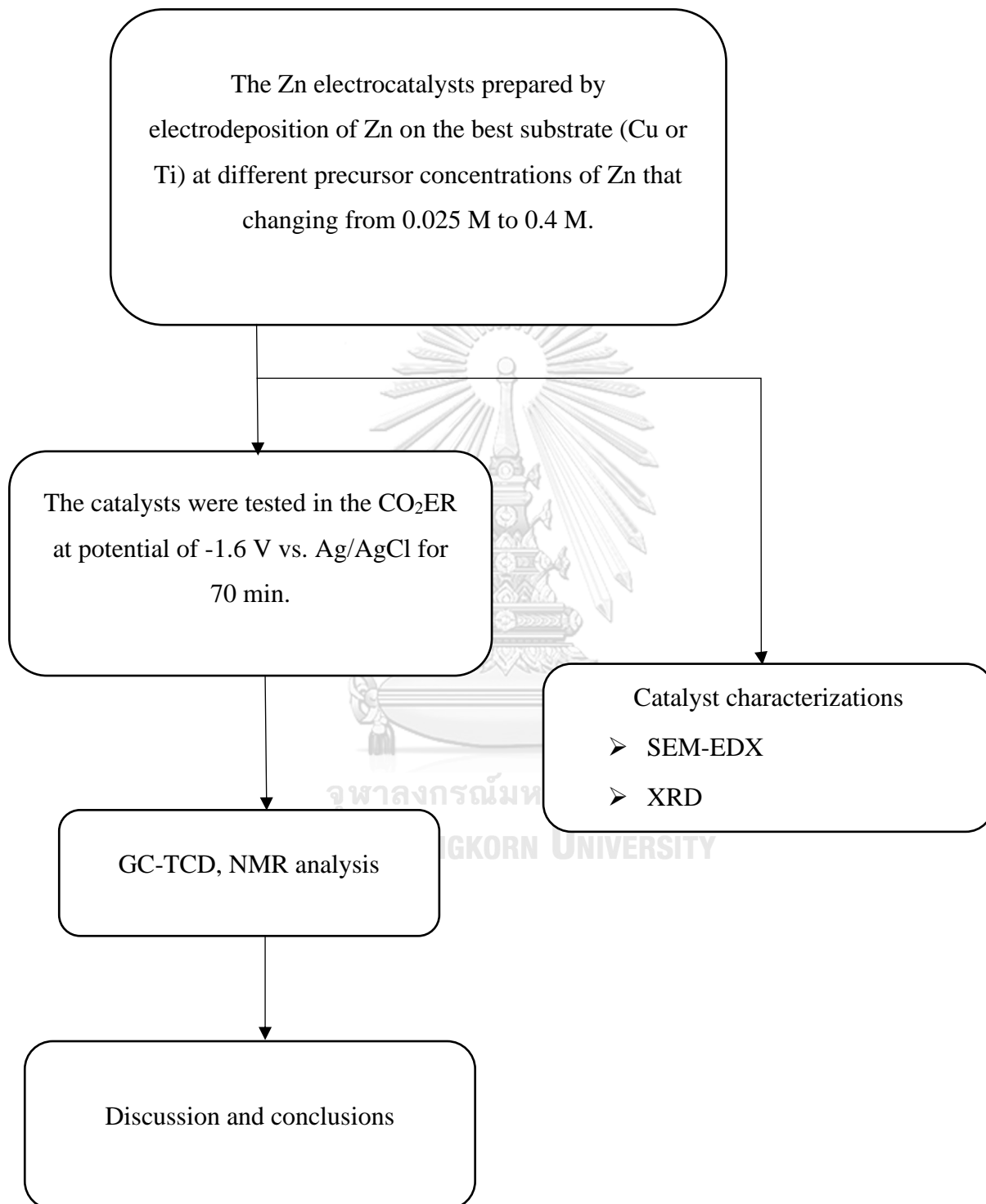
Gas chromatography (Shimadzu GC-2014)	Conditions
Detector	TCD
Column information	Shincarbon ST(50/80)
Carrier gas	Helium (99.999%)
Injector temperature	180°C
Column initial temperature	40°C, Hold time 5 min
Column temperature rate	10°C/min
Column final temperature	200°C
Detector temperature	170°C
Total time analysis	21 min

3.5 Research methodology

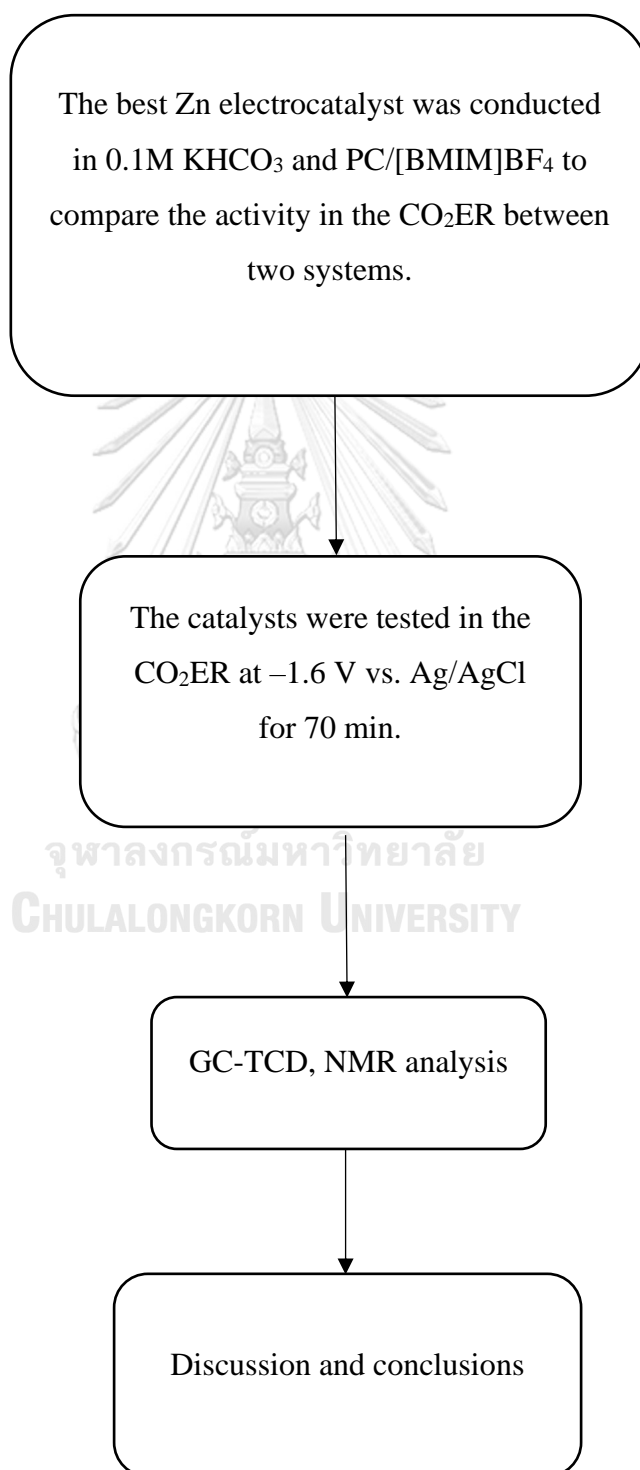
Part I. To study the effects of different substrates (Cu, Ti) on the characteristics and the activity of Zn catalysts in the CO₂ER.



Part II. To investigate the effects of Zn precursor concentrations, by using the better substrate from Part I, on the characteristics and the activity in the CO₂ER.



Part III. To compare the activity in the CO₂ER between KHCO₃ aqueous solution and ionic liquid (PC[BMIM]BF₄) system, using the best Zn electrocatalyst from Part II



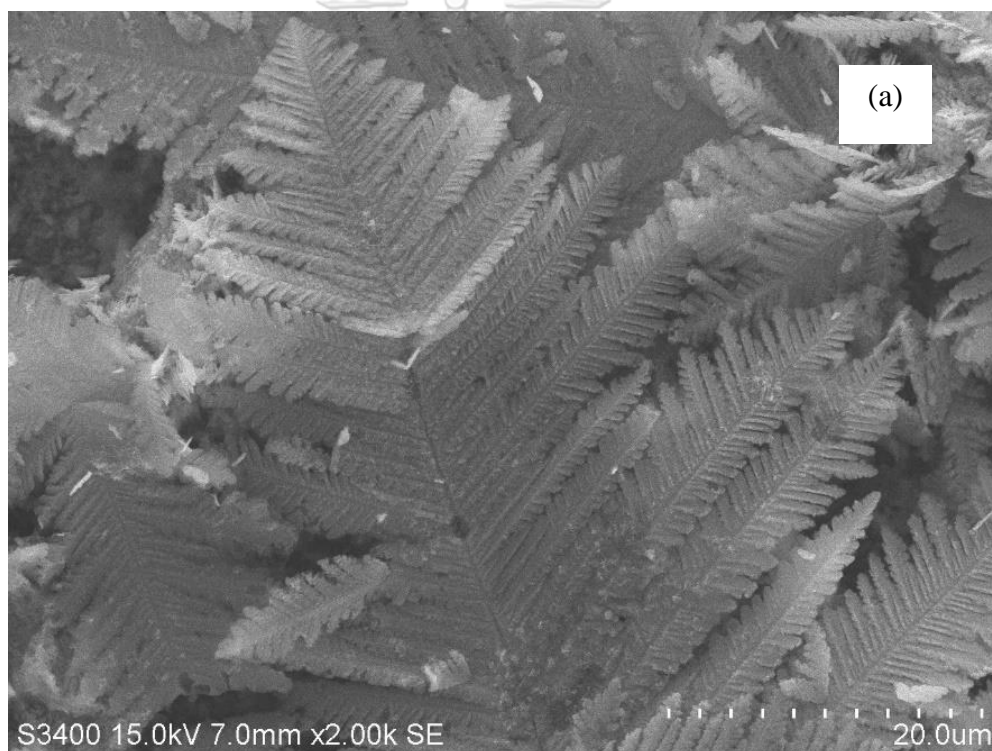
CHAPTER IV

RESULTS AND DISCUSSION

Part I. To study the characteristics and the CO₂ER performances of Zn electrocatalysts prepared by Zn electrodeposition on different substrates (Cu, Ti).

4.1 Characterization of Zn electrocatalysts on different substrates (Cu, Ti)

4.1.1 Scanning electron microscope-energy dispersive X-ray spectroscopy (SEM-EDX) of 0.05Zn/Cu and 0.05Zn/Ti



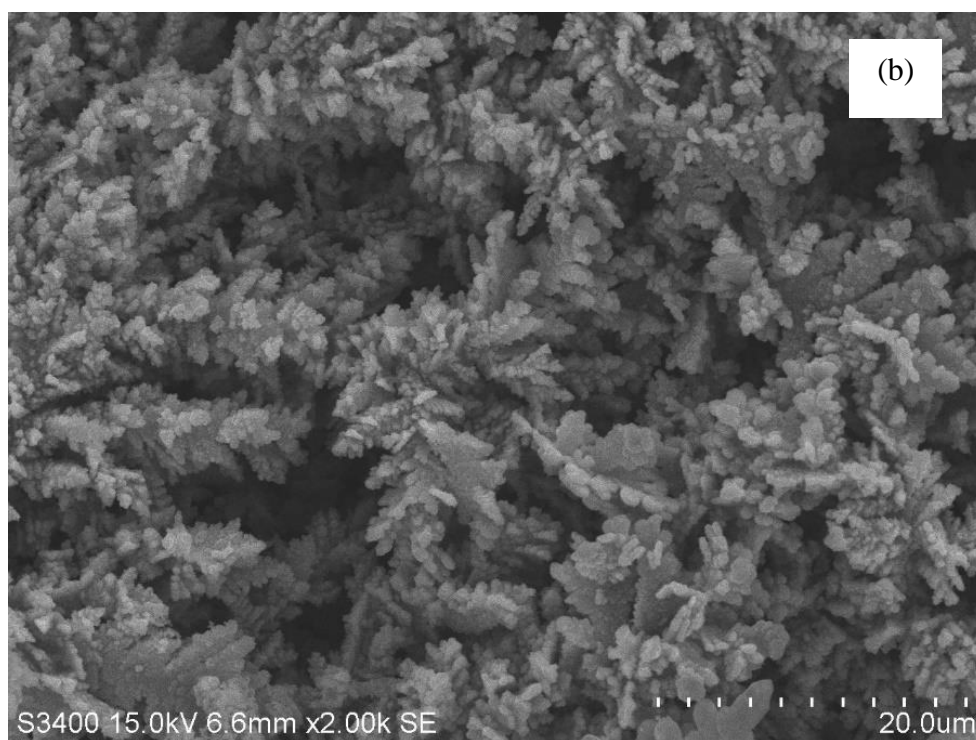


Figure 8. SEM images of (a) 0.05Zn/Cu and (b) 0.05Zn/Ti.

Table 12. Percent by atom of 0.05Zn/Cu and 0.05Zn/Ti.

Catalyst	Percent by atom		
	Zn (%)	Cu or Ti (%)	O (%)
0.05Zn/Cu	80.2	3.4	16.5
0.05Zn/Ti	95.8	1.2	3.0

Firstly, the obtained catalysts from electrodeposition of Zn on different substrates were investigated how the substrates affect the morphologies of the prepared electrocatalysts. Figure 8a and Figure 8b show the SEM images of 0.05Zn/Cu and 0.05Zn/Ti, respectively. The electrocatalysts showed the same structures in form of dendrite morphology. These results indicated that the substrates did not affect to the morphology of catalysts but rather depended on concentration of Zn precursor [86]. It was reported from many reports that the formation of dendritic form occurred by the

region at near branches of dendrite structure having a low Zn concentration, so the dendrite is forced to grow into a higher Zn concentration [17, 87]. Comparing the particle size of dendrites, it was found that the particle sizes of 0.05Zn/Ti were bigger than those of 0.05Zn/Cu. Because the particle sizes depended on the deposition rate, the slower deposition rate produces larger particle sizes [17]. Thus, the deposition rate of Zn on Ti was slower than that of Zn on Cu. It suggested that the properties of substrates (e.g., conductivity, type of metal) had influence on ability of deposition. Table 12 shows the percent by atom of Zn that was deposited on each substrate. It was found that the number of deposited Zn atoms on Ti was higher than those of Zn on Cu. According to electrodeposition theory [75], the substrate has lower reduction potential more than the metal precursor, resulting on the lower energy input for deposition. Thus, those Zn atoms prefer to deposit on Ti more than Cu.

4.1.2 X-ray diffraction (XRD) of 0.05Zn/Cu and 0.05Zn/Ti

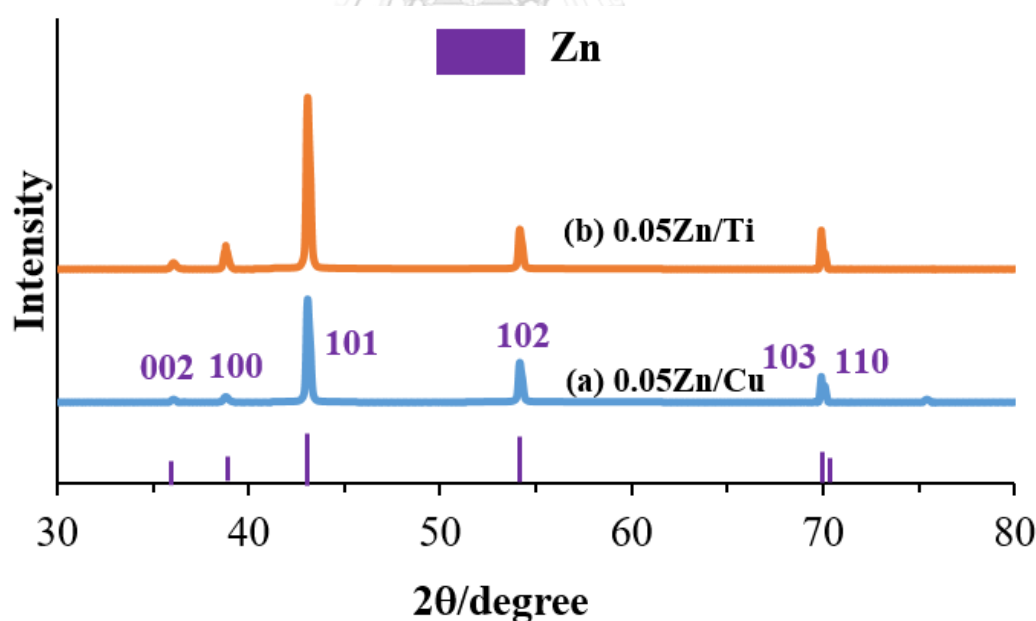


Figure 9. XRD patterns of (a) 0.05Zn/Cu and (b) 0.05Zn/Ti.

Next, the electrocatalysts were investigated by using X-ray diffraction. Figure 9 shows the crystalline structure of 0.05Zn/Cu and 0.05Zn/Ti, obtained from electrodeposition of Zn on substrates (Cu, Ti). Both the diffraction peaks of 0.05Zn/Cu

and 0.05Zn/Ti were exactly aligned with the pattern of pure Zn metal (JCPDS file#: #04-0831), indicating that Zn elements were properly deposited on the substrate. The Zn (101) facet was detected as the major peak at around 43° on both 0.05Zn/Cu and 0.05Zn/Ti. Moreover, it was observed that the intensity of Zn (101) facet of 0.05Zn/Ti was higher than that of 0.05Zn/Cu, corresponding to the decrease in the particle sizes of Zn. This characterization was in good agreement with the SEM images as mentioned above.

4.2 Activity test of Zn electrocatalysts on different substrates (Cu, Ti) in the CO₂ER

Table 13. The catalytic performances of Zn/Cu and Zn/Ti.

Catalyst	Rate (μmol/min)				CO/H ₂ rate ratio	Current (mA)	Faradaic efficiency (FE)
	CO	H ₂	Formate	n-Propanol			CO
0.05Zn/Cu	3.07	1.10	0.17	0.013	2.78	-5.93	83.38%
0.1Zn/Cu	2.27	1.36	0.43	0.021	1.68	-6.22	58.89%
0.05Zn/Ti	0.63	0.90	0.09	0.000	0.70	-2.21	46.26%
0.1Zn/Ti	0.70	1.53	0.10	0.000	0.46	-3.84	29.56%

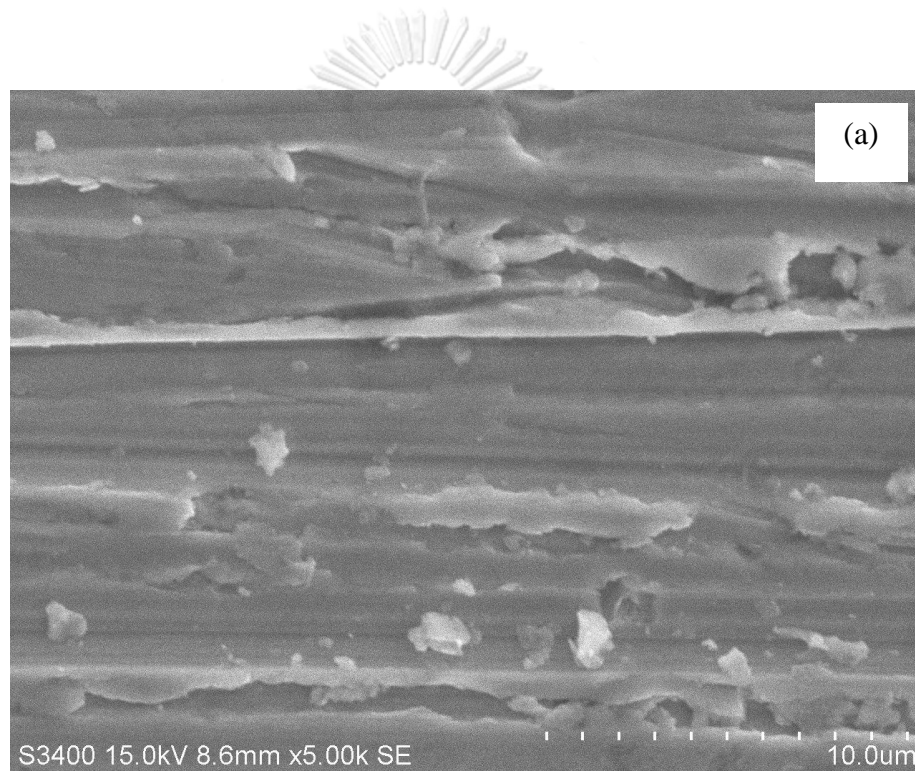
To compare the activity of Zn electrocatalysts with different substrates, all catalysts were tested via the CO₂ER at 1.6 V vs. Ag/AgCl for 70 minutes in CO₂ saturated 0.1 M KHCO₃. The obtained product included CO as a main product, H₂ as a byproduct, and a little amount of liquid products (HCOOH and n-Propanol). The catalytic performances were evaluated in terms of CO/H₂ molar ratio and CO faradaic efficiency (FE) as shown in Table 13. Generally, Zn did not cover all area on surface, which it was possible that the area of gap had influence for competing reaction between CO₂ and substrate. Ti was classified as inert metal in reduction of CO₂. Thus, Ti does not compete with CO₂ reaction [88]. Although the results of characterization of 0.05Zn/Ti showed outstanding features, which has a higher Zn (101) face, which favor on CO production [18] and the higher amount of deposited Zn on substrate. The performances, including the CO/H₂ molar ratio and CO FE of 0.05Zn/Ti were still lower

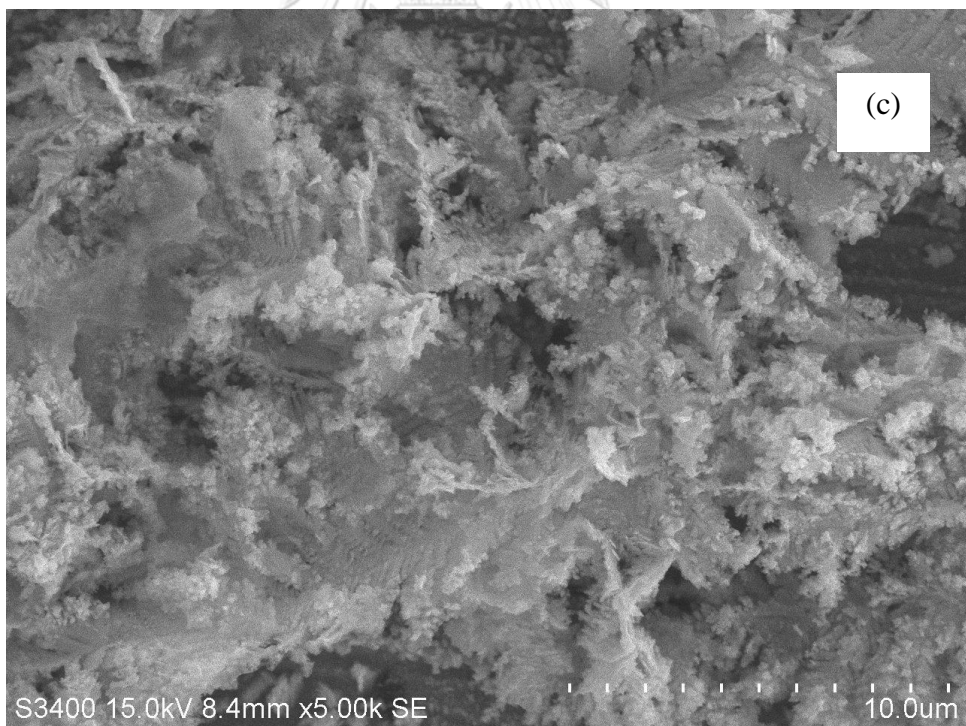
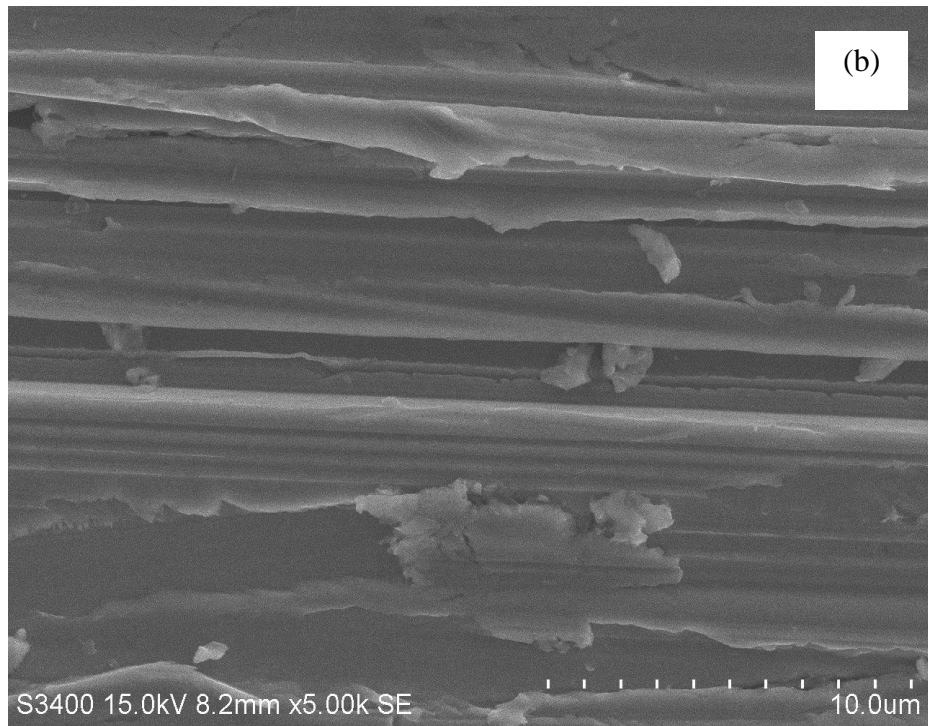
than those of Zn/Cu. As displayed by the low CO/H₂ rate ratio of Zn/Ti, the hydrogen evolution rate was faster than the CO₂ER. This indicated that the deposited Zn on substrate was not main factor on the activity of the CO₂ER. When the current density was considered, it is likely that the property of substrate is the main variable. According to Luo et al. (2014) [71], they used Cu and Ni mesh as a substrate for electrodeposition of Zn. Those results showed that the high %FE CO was achieved from Cu and Ni mesh. It was found that a conductive support boosts the charge electron around surface of catalyst. In case, Ti has a poor conductivity when compared to Cu. Thus, Ti does not improve the activity of Zn electrocatalysts. Moreover, it was observed that n-propanol, which requires 18 electron for reduction [39], was not found in the CO₂ER on Zn/Ti. Because of the high resistant of Ti, the energy input is not enough to overcome the kinetic energy barrier for CO₂ER to n-propanol. In addition, Zn electrocatalyst was tested at Zn concentration of 0.1 M to confirm the results. Both Zn concentration of 0.05 M and 0.1 M on Cu provided the CO FE of 83.38 % and 58.89 %, respectively. These values are around 2 times higher than those of Zn/Ti. Thus, Cu foil was selected as the substrate to further study in the next objective.

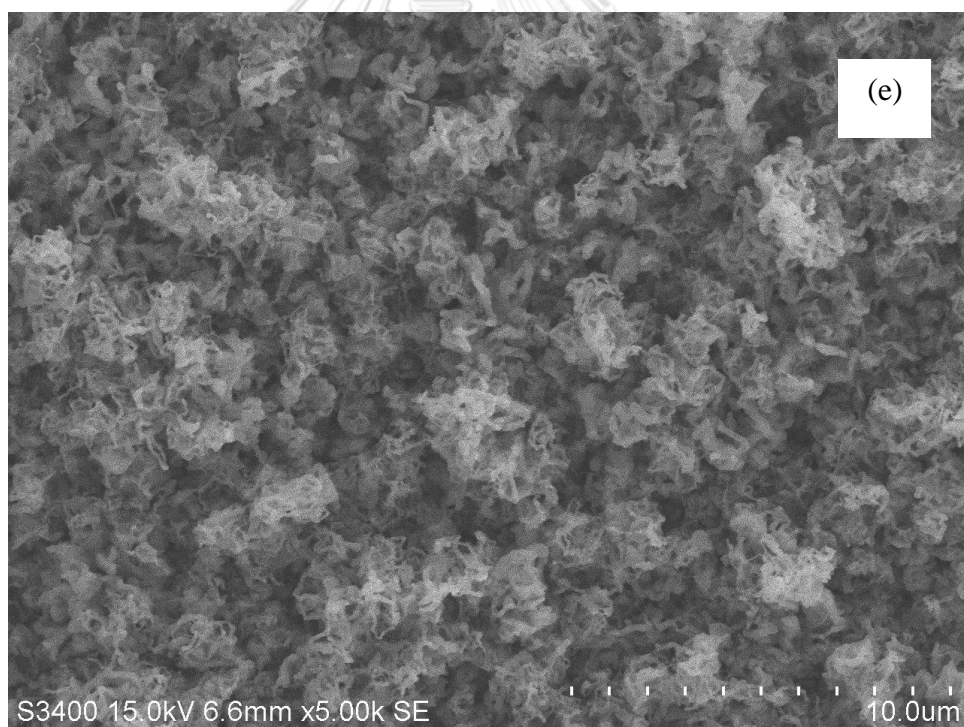
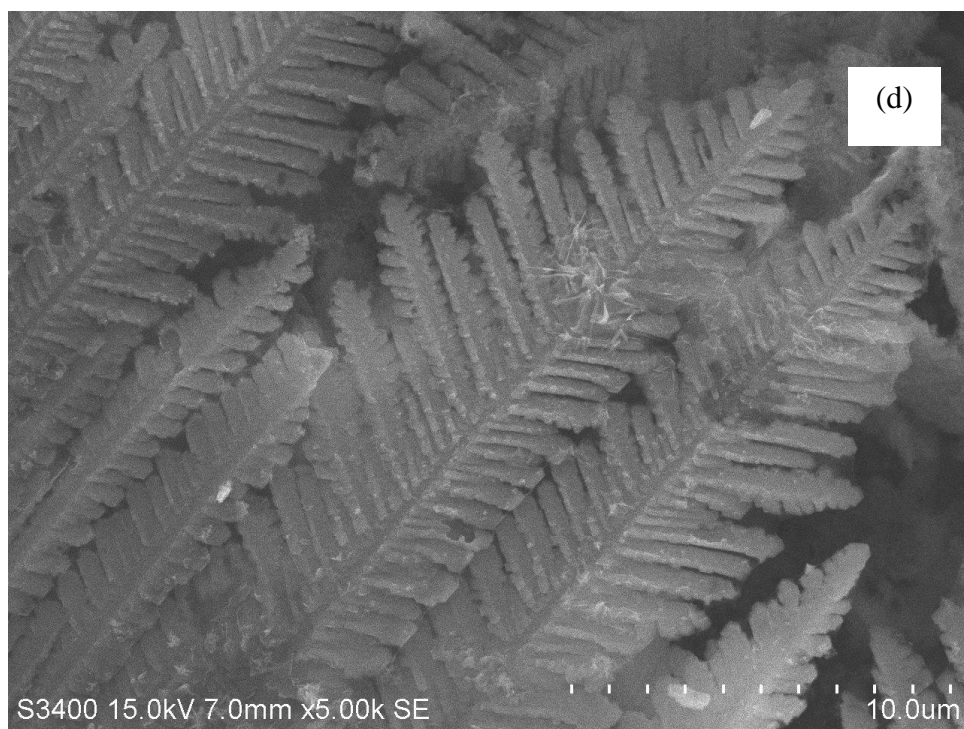
Part II. To investigate the effects of Zn precursor concentration, by using the better substrate from the first objective, on the characteristics and the activity in the CO₂ER.

4.3 Characterization of Zn foil, Cu foil and Zn/Cu prepared with various Zn concentrations

4.3.1 Scanning electron microscope-energy dispersive X-ray spectroscopy (SEM-EDX) of Zn foil, Cu foil, and Zn/Cu at various concentrations







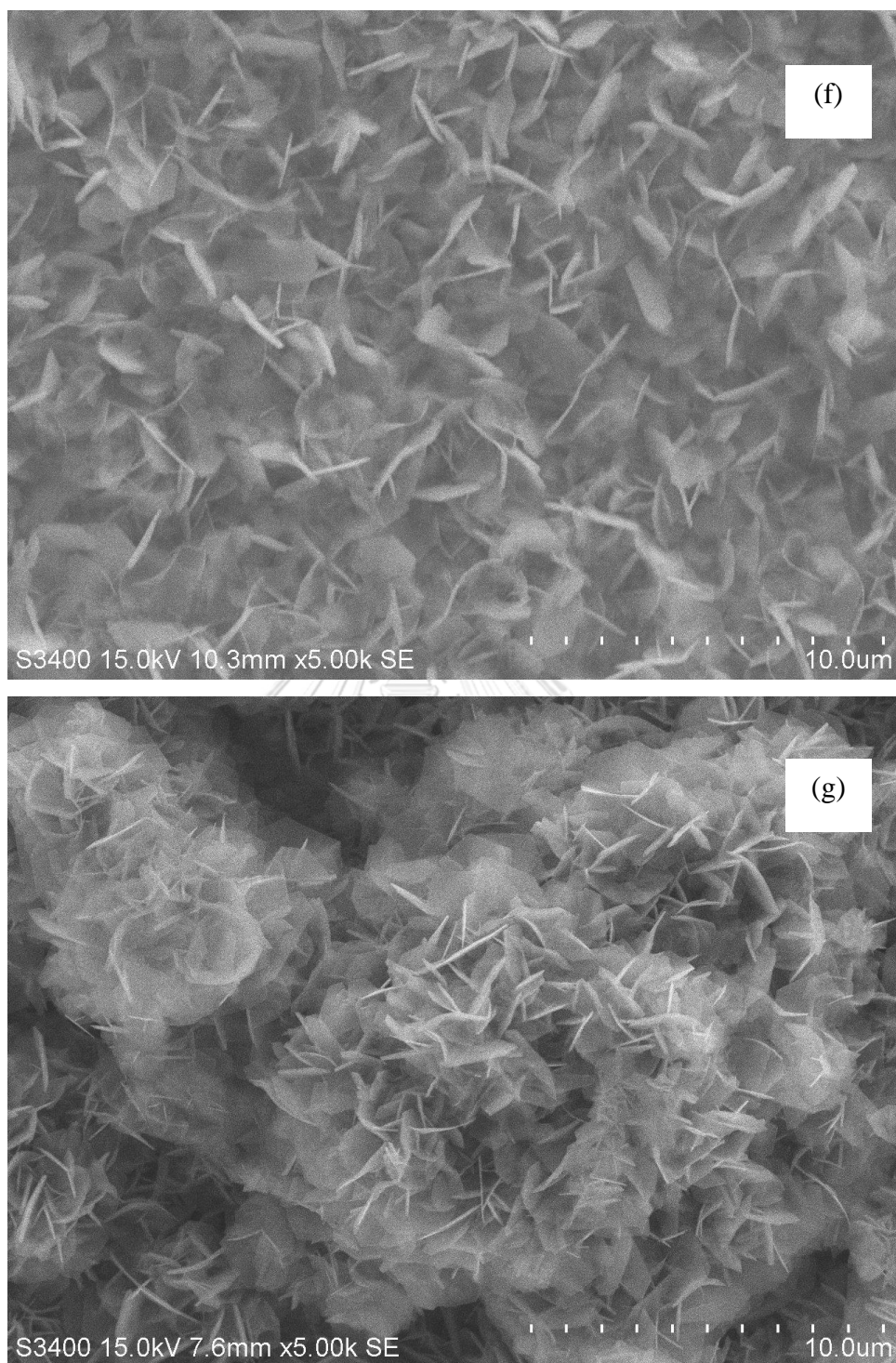


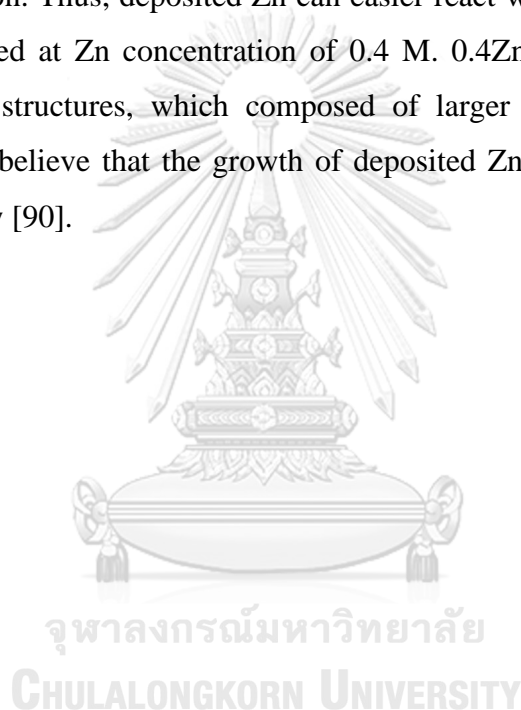
Figure 10. SEM images of (a) Zn foil, (b) Cu foil, (c) 0.025Zn/Cu, (d) 0.05Zn/Cu, (e) 0.1Zn/Cu, (f) 0.2Zn/Cu, and (g) 0.4Zn/Cu.

Table 14. Percent by atom of Zn/Cu at various concentrations.

Catalyst	Percent by atom		
	Zn (%)	Cu (%)	O (%)
0.025Zn/Cu	30.1	62.5	7.5
0.05Zn/Cu	80.2	3.4	16.5
0.1Zn/Cu	94.2	1.9	3.9
0.2Zn/Cu	53.2	9.5	37.3
0.4Zn/Cu	51.3	7.7	41.0

From part I, the better substrate (Cu) was used to study the effect of concentrations of Zn precursor from 0.025 M to 0.4 M. The precursor for deposition included ZnCl₂ and NaCl, which was used as a supporting electrolyte. The obtained catalysts from electrodeposition of Zn at different concentrations were investigated on the morphologies of the prepared electrocatalysts, as shown in Figure 10. From Figure 10a and 10b, surface of Zn foil and Cu foil were similar rock-like layers which these scratches obtained by mechanical polishing. At low concentration of Zn precursor, 0.025Zn/Cu and 0.05Zn/Cu showed the dendritic morphologies, as shown in Figure 10c and 10d, respectively. Appearance of dendrite form was described that the electrodeposition occurred under limitation of mass-transfer [17, 87]. This causes growth of braches of dendrite toward the higher concentration of Zn ions region. It was observed that the number of Zn atoms of 0.025Zn/Cu was lower than that of 0.05Zn/Cu, as shown in Table 14. It was consistent with SEM image (Figure 10c), which Cu surface was seen clearly. This was indicated that the concentration of Zn ions had influence on the deposition rate. The low number of Zn atoms on Cu was occurred from the low deposition rate, which Zn ions hardly diffuse to the electrode surface. When concentration of Zn precursor was increased to 0.1 M, the morphology of Zn was changed from dendritic structure to mossy structure [17], as shown in Figure 10e. The mossy structure contained a high amount of small Zn filaments, obtained from the fast deposition rate. Among various concentrations of Zn precursor, 0.1Zn/Cu provided the highest number of Zn atoms. Thus, the 0.1Zn/Cu would provide the highest surface area. In contrast, increasing of Zn concentration to 0.2 M and 0.4 M resulted in the low

number of Zn atoms. Because there are large amount of zinc oxide (ZnO), shown in form of porous structure. 0.2Zn/Cu (Figure 10f) showed the sheet-like foam structures, containing a numerous of pores [89]. The formation of ZnO was believed to occur from hydrogen evolution as a competitive reaction. The high number of Zn ions resulted in the high conductivity. Thus, a large number of H₂ bubbles were generated. The molecules of H₂ acted as a template during electrodeposition of Zn catalyst. Thus, the metal ions were obstructed from H₂ bubbles and generated as porous structure. For the other hypothesis, the high number of Cl⁻ would chelate with Zn ions, resulting in the slow rate deposition. Thus, deposited Zn can easier react with H₂O. The formation of ZnO was confirmed at Zn concentration of 0.4 M. 0.4Zn/Cu (Figure 10g) showed sphere-like foam structures, which composed of larger pores when compared to 0.2Zn/Cu. It was believe that the growth of deposited Zn was formed to keep their surface energy low [90].



4.3.2 X-ray diffraction (XRD) of Zn foil, Cu foil, and Zn/Cu at various concentrations.

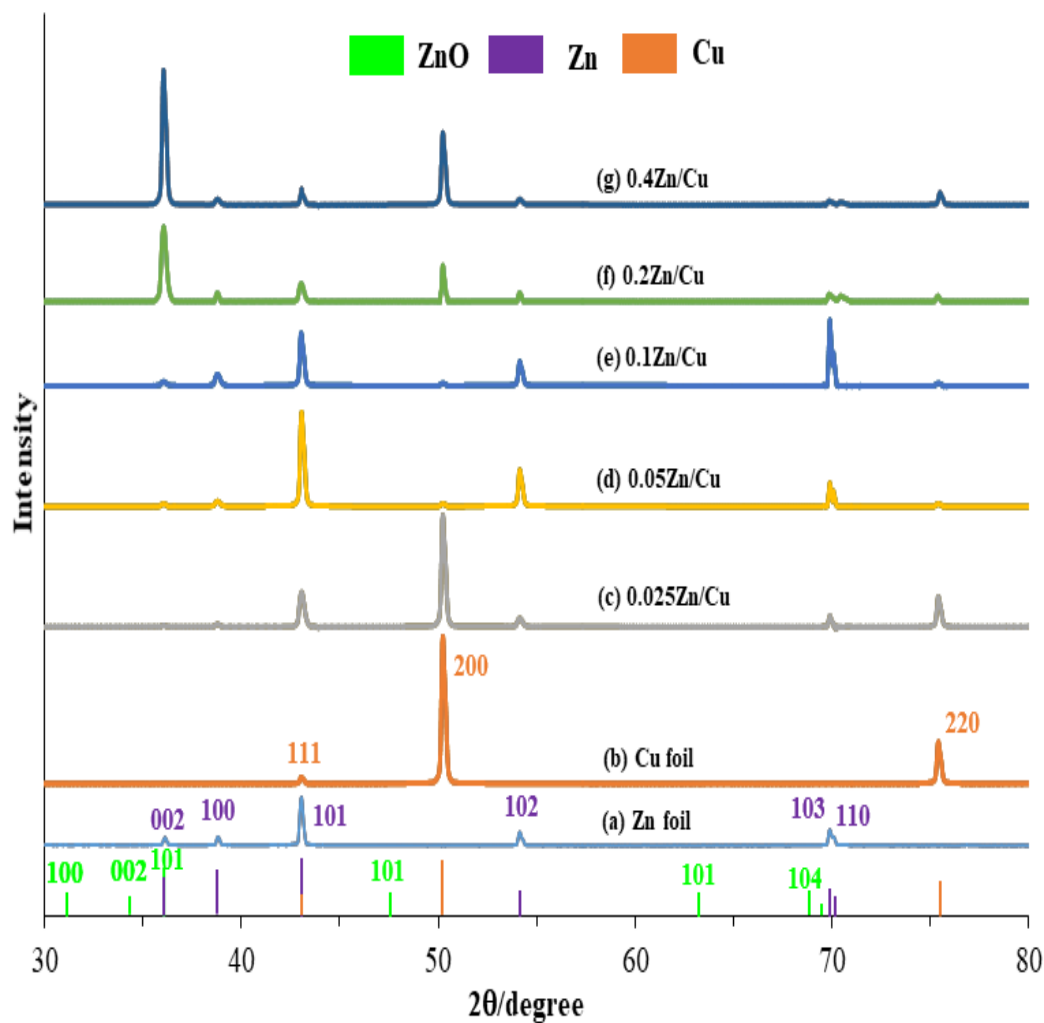


Figure 11. XRD patterns of (a) Zn foil, (b) Cu foil, (c) 0.025Zn/Cu, (d) 0.05Zn/Cu, (e) 0.1Zn/Cu, (f) 0.2Zn/Cu, and (g) 0.4Zn/Cu.

The XRD measurement of the Zn catalysts at different concentrations were carried out to analyze the crystal structure of Zn deposited. Figure 11 shows the crystalline structure of Zn foil, Cu foil, and Zn/Cu at various concentrations. Figure 11a and 11d show Zn foil and 0.05Zn/Cu, which had the Zn (101) at 43.1° as dominant peak, it indicated that the composition in samples consisted of pure Zn. Figure 11b

shows Cu foil, which had the Cu (200) at 50.2° as dominant peak, it indicated that the composition contained pure Cu. When Zn was deposited on Cu, the intensity of peak at 50.2° and 75.4°, corresponding to both the Cu (200) and Cu (220) face would be decreased. As Figure 11c, 0.025Zn/Cu showed Cu (200) and Cu (220) as main peak, indicating that the deposited Zn was not covered all area of the substrate. At Zn concentration of 0.1 M, it was found that the intensity of Zn (101) was decreased while peak at 70.2°, corresponding to Zn (103) was increased. This was described that the Zn particles rearranged. Moreover, peak at 36°, corresponding to Zn (002) face and ZnO (101) face, became dominant peak for 0.2Zn/Cu and 0.4Zn/Cu. This indicated that the large number of ZnO favor on porous structures. It was suggested that the sheet-like structure occurred from bonding of Cl ions and hexagonal wurtzite on (0001) and (100) families of planes, respectively [91].

4.4 Activity test of Zn electrocatalysts of Zn foil, Cu foil and Zn/Cu prepared with various Zn concentrations

Table 15. The catalytic performances of Zn foil, Cu foil and Zn/Cu prepared with various Zn concentrations.

Catalyst	Rate ($\mu\text{mol}/\text{min}$)				CO/H ₂ rate ratio	Current (mA)	Faradaic efficiency (FE)
	CO	H ₂	Formate	n-Propanol			CO
Zn foil	0.66	0.29	0.12	0.004	2.25	-1.85	57.42%
Cu foil	0.44	3.69	0.35	0.065	0.12	-5.60	12.57%
0.025MZn/Cu	0.58	2.15	0.20	0.037	0.27	-4.18	22.53%
0.05MZn/Cu	3.07	1.10	0.17	0.013	2.78	-5.93	83.38%
0.1MZn/Cu	2.27	1.36	0.43	0.021	1.68	-6.22	58.89%
0.2MZn/Cu	1.83	2.73	0.14	0.002	0.67	-6.21	47.42%
0.4MZn/Cu	1.69	2.82	0.09	0.004	0.60	-7.23	37.77%

To compare the activity of electrocatalysts, all the catalysts were tested via the CO₂ER at 1.6 V vs. Ag/AgCl for 70 minutes in CO₂ saturated 0.1 M KHCO₃. The obtained product included CO as a main product, H₂ as a byproduct, and a little amount of liquid products (HCOOH and n-propanol). The catalytic performances were evaluated in terms of CO/H₂ molar ratio and %FE CO, as shown in Table 15. The CO/H₂ rate ratio and the CO FE of Zn foil were higher than those of Cu foil, indicating

that Zn foil suppress the HER. Because of the high resistant and weak binding of CO, CO was rapidly produced on surface of catalyst [88]. Although CO/H₂ rate ratio of Cu foil would be low, it was possible that CO was converted into liquid products (formate and n-propanol) on Cu foil substrate. Because of the low resistant of Cu, it resulted the higher current density than Zn foil. Thus, most of CO on Cu foil can be easily converted into formate and n-propanol. As the concentrations of Zn precursor were varied, it was found that the highest CO/H₂ rate ratio and %FE CO were achieved on 0.05Zn/Cu. Because of the large the number of deposited Zn atoms and the highest intensity of Zn (100) facet, which favor CO production [18]. The other hypothesis is that the dendrite structure, which contains numerous stepped sites, that suppress hydrogen evolution [17]. Although 0.025Zn/Cu have the same morphology, compared to 0.05Zn/Cu, the area of Cu remained higher than the deposited Zn. This caused the values of CO/H₂ rate ratio and %FE CO, which were similar to Cu foil. However, for 0.1Zn/Cu, it was found that it provided the highest surface area, caused by the decrease in particle size of deposited Zn. As a consequence, the CO/H₂ rate ratio and %FE CO of 0.1Zn/Cu were lower than 0.05 Zn/Cu. It was believed that increasing of the surface area might be not enough to improve CO₂ reduction [58]. According to previous works, Kanan found that the different structure affect to the CO selectivity on Cu foil [92] and Chorkendorff et al. also suggested that roughness of surface affect to CO₂ activity [93]. It may be possible that more rough surface would lead to higher low-coordinated active sites, which help to achieve high production of formate. Moreover, these low-coordinated sites tightly bond with CO₂ molecules, resulting in higher activity. When the concentrations of Zn precursor were higher than 0.1 M, a large amount of ZnO occurred on the surface of Zn. According to the XRD in Figure 11, the Zn (002) and ZnO (101) facet show dominant peaks than Zn (100) facet. Thus, the CO/H₂ rate ratio and %FE CO of 0.2Zn/Cu and 0.4Zn/Cu were decreased. This indicated that the active facets on surface of catalysts play an important role on the catalytic performances. Among the prepared Zn electrocatalysts, the 0.05Zn/Cu provided the highest of CO/H₂ rate ratio and %FE CO at 2.78 and 83.38%, respectively. Moreover, the %FE CO of 0.05Zn/Cu was 1.5 times higher than that Zn foil. It was indicated that dendritic structure of Zn enable for the CO₂ER. In addition, the CO₂ER activity also depends on electrolyte. The

use of ionic liquids may improve the %FE CO of Zn catalysts. Thus, the best Zn catalyst were tested further in IL in part III.

Part III. To analyze the CO₂ER activity between the reaction passing in aqueous electrolyte and ionic liquid (IL) with the best Zn electrocatalyst.

4.5 Electrochemical measurement of 0.05Zn/Cu in 0.1 M KHCO₃ and ionic liquid (PC/[BMIM]BF₄)

4.5.1 Linear sweep voltammetry (LSV) of 0.05Zn/Cu in 0.1 M KHCO₃ and ionic liquid (IL)

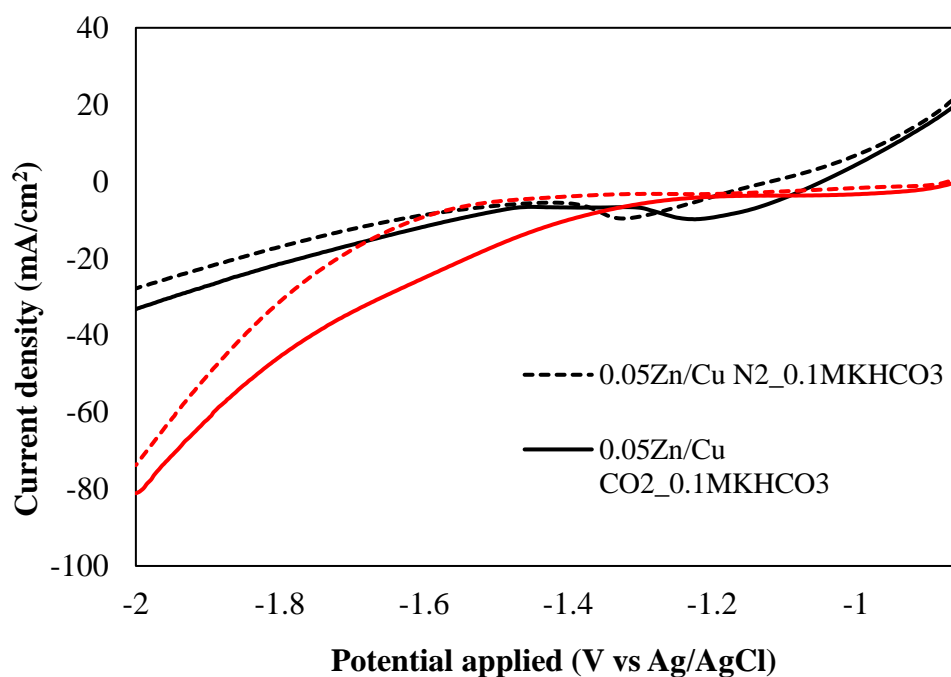


Figure 12. LSV curves of 0.05Zn/Cu in N₂ and CO₂ saturated solutions (0.1M KHCO₃ and IL) with a scan rate 100 mV/s.

To evaluate the ability of the CO₂ER on 0.05Zn/Cu in 0.1 M KHCO₃ and IL, linear sweep voltammetry (LSV) was applied under N₂ and CO₂ saturated solutions. As shown in Figure 12, dash lines and thick lines corresponded to rate of hydrogen evolution reaction (HER) and rate of the CO₂ER. At potential of -1.6 V vs Ag/AgCl, the gap

between these lines, which related to rate of products, in 0.1 M KHCO_3 was larger than in IL. It suggested that 0.05Zn/Cu in IL had a higher catalytic activity than in 0.1 M KHCO_3 over studied potentials. Among the cathodic potentials from -0.85 V to -2 V vs Ag/AgCl, It was seen that the reaction in IL had an onset potential around -1.3 V, which it was shifted more positive when compared with those in 0.1 M KHCO_3 . Thus, the high conductivity in IL contributed to lower energy consumption. This could be explained by the fact that IL allows CO_2 to conveniently transport to the cathode. These results were similar with previous work [94]. Moreover, reduction peak was found in 0.1 M KHCO_3 . It occurred from a little amount of ZnO that was reduced into Zn form. Thus, in 0.1 M KHCO_3 allowed the decreasing in oxide layer on catalyst.

4.5.2 Comparison of the activity tests of 0.05Zn/Cu in 0.1 M KHCO_3 and IL.

Table 16. The catalytic performances of 0.05Zn/Cu in 0.1 M KHCO_3 and IL.

Catalyst	Rate ($\mu\text{mol}/\text{min}$)				CO/H ₂ rate ratio	Current (mA)	Faradaic efficiency (FE)
	CO	H ₂	Formate	n-Propanol			CO
0.05Zn/Cu_0.1M KHCO_3	3.07	1.10	0.63	0.013	2.78	-5.93	83.38%
0.05Zn/Cu_IL	1.42	0.31	-	-	4.55	-4.53	50.73%

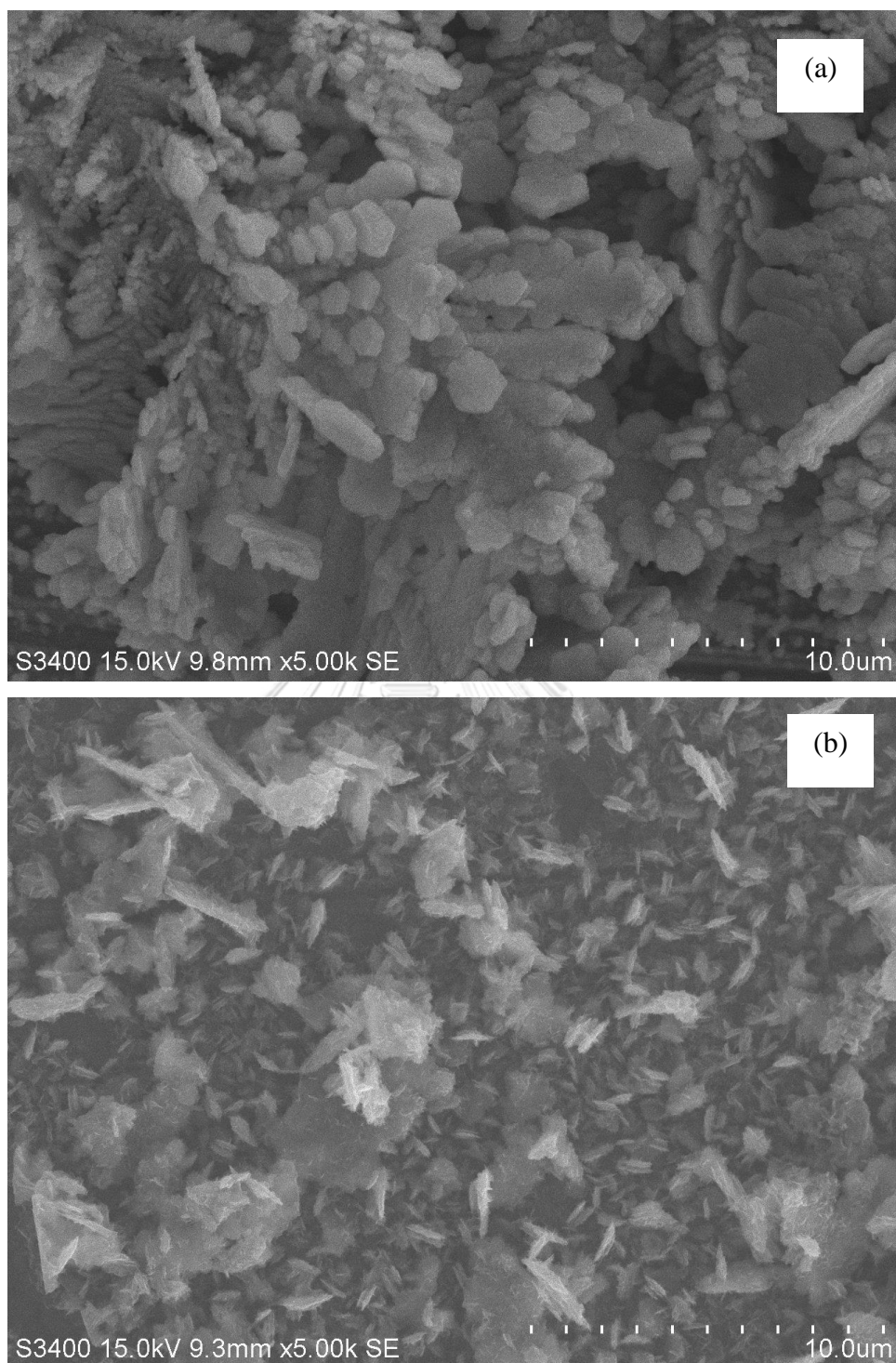


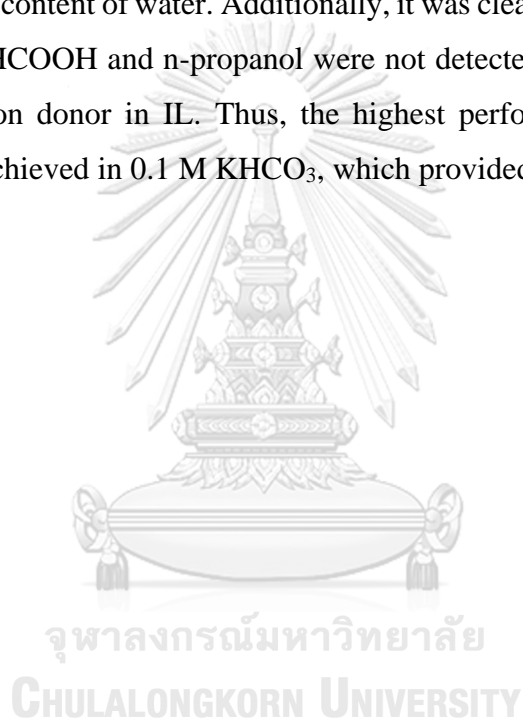
Figure 13. SEM images of (a) 0.05Zn/Cu in 0.1M KHCO_3 and (b) 0.05Zn/Cu in IL after run reaction.

Table 17. Percent by atom of 0.05Zn/Cu after run reaction in 0.1M KHCO₃ and IL.

Catalyst	Percent by atom		
	Zn (%)	Cu (%)	O (%)
0.05Zn/Cu_0.1M KHCO ₃	95.2	3.3	1.6
0.05Zn/Cu_IL	11.7	76.2	12.1

To understand the effects of electrolytes, 0.05Zn/Cu were tested in CO₂ saturated 0.1 M KHCO₃ and ionic liquid, containing PC, [BMIM]BF₄, and water (5:4:1 by volume ratio) at -1.6 V vs. Ag/AgCl for 70 minutes. The obtained product included CO as a main product, H₂ as a byproduct, and a little amount of liquid products (HCOOH and n-propanol). The catalytic performances were evaluated in terms of CO/H₂ molar ratio and % FE CO, as shown in Table 15. When comparing the activities of CO₂ER on 0.05Zn/Cu in aqueous electrolyte and ionic liquid (IL), it was found that the % FE CO from the reaction in aqueous electrolyte was higher than that carried out in ionic liquid mixture. According to the outstanding role of IL, while the CO₂ER was occurring, the IL, behaving like a surfactant, which will adsorb on cathode surface before, then will stabilize CO₂⁻ radical anions, contributing to the formation of CO [95]. It was possible that while IL molecules shifting down to adsorb on catalyst surface. It was hit with too high force, resulting the falling of deposited Zn from catalyst surface. This evidence was confirmed by SEM in Figure 13. As shown in Figure 13a, the morphology of Zn after run in aqueous electrolyte was the same before, which it appeared in form of dendrite structure but the size of dendrites were increased from 0.4 μm to 1 μm. For the Zn catalyst after CO₂ER in IL, the morphology of Zn showed a low content of dendrites, which indicated partial loss of some Zn from the substrate. When comparing the Zn catalysts after run reactions between in IL and aqueous solution, it was found that in IL, the Zn catalyst had much lower amount of deposited Zn (11.7 %) as compared to that deposited Zn before reaction (80.2%), as shown in Table 16. On the other hand, in 0.1 M KHCO₃, it was found that there was increasing number of deposited Zn (95.2%). It was likely that Zn clusters were dissolved and

redeposited on the substrate more densely, according to a previous work [17]. This phenomenon pointed out that deposited Zn may be unstable in IL because the properties of IL such as a viscosity of [BMIM]BF₄. In this study, the ratio by volume of PC, [BMIM]BF₄ and H₂O was selected from a previous work using Ag catalysts [85]. This ratio may be not suitable for Zn catalyst. The high viscosity of [BMIM]BF₄ may cause high surface tension, and Zn could be eroded by the IL. Considering the CO/H₂ ratio, it was found that the CO/H₂ ratio of the CO₂ conversion in IL were higher than that of the CO₂ conversion in 0.1 M KHCO₃. It is suggested that the IL suppressed the HER because of a lower content of water. Additionally, it was clearly observed that the liquid products such as HCOOH and n-propanol were not detected in IL, which was caused by a lack of proton donor in IL. Thus, the highest performance of the CO₂ER on 0.05Zn/Cu were achieved in 0.1 M KHCO₃, which provided the %FE CO of 83.38%.



CHAPTER V

CONCLUSIONS

5.1 Conclusions

Electrochemical reduction of CO₂ (CO₂ER) to CO using Zn electrocatalysts was investigated under various conditions at ambient conditions in an H-cell type reactor. Firstly, the effect of substrates (Cu, Ti) on the characteristics and the CO₂ER performances of Zn electrocatalysts were studied. The results show that the concentration of Zn precursor during electrodeposition on different substrates had no influence on the morphology of Zn structures. Although the 0.05Zn/Ti had the higher number of the deposited Zn than the 0.05Zn/Cu, the use of Ti as the substrate still provided the lower % FE CO than those prepared on Cu substrate. Accordingly, the main factor, which plays a role on the performance of the CO₂ER on these catalysts, is the conductivity of substrate. The high conductivity allows easier electron transfer between cathode surface and the electrolyte.

Next, the electrodeposition conditions with various Zn precursor concentrations ranging between 0.025 M to 0.4 M on the characteristics and the activity in the CO₂ER of Zn/ Cu were investigated. At low concentrations of Zn precursor (0.025 M and 0.05M), similar morphology in the form of dendrite structure was observed. Increasing Zn precursor concentration to 0.1 M, the morphology changed into high surface area mossy structure. Because the higher amount of ions was proportional to the deposition rate, the mossy structure had the highest amount of Zn deposited. On the contrary, at concentrations of Zn precursor higher than 0.1 M, lower amount of Zn was deposited due probably to the faster in the H₂ evolution rate. Then, oxide layer could covered Zn surface, which impeded the performances of the CO₂ER. The highest of %FE CO was obtained on the 0.05 Zn/Cu and was attributed to the presence of the strong appearance of Zn (101) facet.

Finally, the CO₂ER activity between the reaction passing in aqueous electrolyte (0.1 M KHCO₃) and ionic liquid (PC, [BMIM]BF₄, H₂O) on the best Zn catalyst were evaluated. The LSV results showed that the reaction in ionic liquid (IL) started to occur at lower potential than the reaction in aqueous solution due to the better CO₂

transport to cathode surface in IL. Despite the high conductivity of IL, the obtained %FE CO in IL was lower than that in aqueous electrolyte. This was probably because erosion of Zn occurred under IL. Moreover, the Zn clusters after run reaction in aqueous solution could redeposit on the substrate. Thus, the highest %FE CO was achieved in 0.1 M KHCO_3 on 0.05Zn/Cu (83.38%), which was about 1.5 times higher compared to Zn foil (57.42%).

5.2 Recommendations

1. The increasing of surface area of deposited electrocatalysts need to be confirmed by electrochemical measurement.
2. The in-situ characterization of electrocatalysts should be used to decrease error from oxidation of Zn in air
3. The volume ratio of PC $[\text{BMIM}]\text{BF}_4$ and water should be further studied to find the suitable conditions for Zn catalyst.

REFERENCES

1. Lu, Y., et al., *Efficient electrocatalytic reduction of CO₂ to CO on an electrodeposited Zn porous network*. *Electrochemistry Communications*, 2018. **97**: p. 87-90.
2. Beer, C., et al., *Terrestrial gross carbon dioxide uptake: global distribution and covariation with climate*. *Science*, 2010. **329**(5993): p. 834-838.
3. Shi, J., et al., *Enzymatic conversion of carbon dioxide*. *Chemical Society Reviews*, 2015. **44**(17): p. 5981-6000.
4. Li, K., B. Peng, and T. Peng, *Recent advances in heterogeneous photocatalytic CO₂ conversion to solar fuels*. *ACS Catalysis*, 2016. **6**(11): p. 7485-7527.
5. Lin, L., et al., *The visible-light-assisted thermocatalytic methanation of CO₂ over Ru/TiO (2-x) Nx*. *Applied Catalysis B: Environmental*, 2017. **204**: p. 440-455.
6. Zhan, W., L. Sun, and X. Han, *Recent progress on engineering highly efficient porous semiconductor photocatalysts derived from Metal-organic frameworks*. *Nano-micro letters*, 2019. **11**(1): p. 1.
7. Costentin, C., M. Robert, and J.-M. Savéant, *Catalysis of the electrochemical reduction of carbon dioxide*. *Chemical Society Reviews*, 2013. **42**(6): p. 2423-2436.
8. Whipple, D.T. and P.J. Kenis, *Prospects of CO₂ utilization via direct heterogeneous electrochemical reduction*. *The Journal of Physical Chemistry Letters*, 2010. **1**(24): p. 3451-3458.
9. Ma, S. and P.J. Kenis, *Electrochemical conversion of CO₂ to useful chemicals: current status, remaining challenges, and future opportunities*. *Current Opinion in Chemical Engineering*, 2013. **2**(2): p. 191-199.
10. Zhan, Z. and L. Zhao, *Electrochemical reduction of CO₂ in solid oxide electrolysis cells*. *Journal of Power Sources*, 2010. **195**(21): p. 7250-7254.
11. Dry, M.E., *The fischer-tropsch process: 1950-2000*. *Catalysis today*, 2002. **71**(3-4): p. 227-241.
12. van de Loosdrecht, J. and J. Niemantsverdriet, *Synthesis gas to hydrogen, methanol, and synthetic fuels*, in *Chemical energy storage*. 2012, Walter de Gruyter GmbH. p. 443-458.
13. Koppenol, W. and J. Rush, *Reduction potential of the carbon dioxide/carbon dioxide radical anion: a comparison with other C1 radicals*. *Journal of Physical Chemistry*, 1987. **91**(16): p. 4429-4430.
14. Paik, W., T. Andersen, and H. Eyring, *Kinetic studies of the electrolytic reduction of carbon dioxide on the mercury electrode*. *Electrochimica Acta*, 1969. **14**(12): p. 1217-1232.
15. Jeon, H.S., et al., *Operando evolution of the structure and oxidation state of size-controlled Zn nanoparticles during CO₂ electroreduction*. *Journal of the American Chemical Society*, 2018. **140**(30): p. 9383-9386.
16. Nguyen, D.L.T., et al., *Selective CO₂ reduction on zinc electrocatalyst: the effect of zinc oxidation state induced by pretreatment environment*. *ACS Sustainable Chemistry & Engineering*, 2017. **5**(12): p. 11377-11386.
17. Rosen, J., et al., *Electrodeposited Zn dendrites with enhanced CO selectivity for electrocatalytic CO₂ reduction*. *Acs Catalysis*, 2015. **5**(8): p. 4586-4591.

18. Won, D.H., et al., *Highly efficient, selective, and stable CO₂ electroreduction on a hexagonal Zn catalyst*. *Angewandte Chemie International Edition*, 2016. **55**(32): p. 9297-9300.
19. Gomes, A. and M. da Silva Pereira, *Pulsed electrodeposition of Zn in the presence of surfactants*. *Electrochimica Acta*, 2006. **51**(7): p. 1342-1350.
20. Popov, K., D. Keča, and M. Andjelić, *Electrodeposition of zinc on copper from alkaline zincate solutions*. *Journal of Applied Electrochemistry*, 1978. **8**(1): p. 19-23.
21. Masri, M. and A. Mohamad, *Effect of adding potassium hydroxide to an agar binder for use as the anode in Zn–air batteries*. *Corrosion Science*, 2009. **51**(12): p. 3025-3029.
22. Leung, P., et al., *Zinc deposition and dissolution in methanesulfonic acid onto a carbon composite electrode as the negative electrode reactions in a hybrid redox flow battery*. *Electrochimica Acta*, 2011. **56**(18): p. 6536-6546.
23. Lehr, I. and S. Saidman, *Influence of sodium bis (2-ethylhexyl) sulfosuccinate (AOT) on zinc electrodeposition*. *Applied surface science*, 2012. **258**(10): p. 4417-4423.
24. Singh, M.R., et al., *Hydrolysis of electrolyte cations enhances the electrochemical reduction of CO₂ over Ag and Cu*. *Journal of the American Chemical Society*, 2016. **138**(39): p. 13006-13012.
25. de Salles Pupo, M.M. and R. Kortlever, *Electrolyte effects on the electrochemical reduction of CO₂*. *ChemPhysChem*, 2019. **20**(22): p. 2926.
26. Feng, J., et al., *CO₂ electroreduction in ionic liquids: a review*. *Chinese Journal of Chemistry*, 2018. **36**(10): p. 961-970.
27. Zhang, S., et al., *Ionic liquid-based green processes for energy production*. *Chemical Society Reviews*, 2014. **43**(22): p. 7838-7869.
28. Zeng, S., et al., *Ionic-liquid-based CO₂ capture systems: structure, interaction and process*. *Chemical reviews*, 2017. **117**(14): p. 9625-9673.
29. Hapiot, P. and C. Lagrost, *Electrochemical reactivity in room-temperature ionic liquids*. *Chemical reviews*, 2008. **108**(7): p. 2238-2264.
30. Liu, H., Y. Liu, and J. Li, *Ionic liquids in surface electrochemistry*. *Physical Chemistry Chemical Physics*, 2010. **12**(8): p. 1685-1697.
31. MacFarlane, D.R., et al., *Ionic liquids and reactions at the electrochemical interface*. *Physical Chemistry Chemical Physics*, 2010. **12**(8): p. 1659-1669.
32. Zhang, G.-R. and B.J. Etxold, *Ionic liquids in electrocatalysis*. *Journal of Energy Chemistry*, 2016. **25**(2): p. 199-207.
33. Bard, A., *Standard potentials in aqueous solution*. 2017: Routledge.
34. Leitner, W., *Carbon dioxide as a raw material: the synthesis of formic acid and its derivatives from CO₂*. *Angewandte Chemie International Edition in English*, 1995. **34**(20): p. 2207-2221.
35. Benson, E.E., et al., *Electrocatalytic and homogeneous approaches to conversion of CO₂ to liquid fuels*. *Chemical Society Reviews*, 2009. **38**(1): p. 89-99.
36. Chaplin, R. and A. Wragg, *Effects of process conditions and electrode material on reaction pathways for carbon dioxide electroreduction with particular reference to formate formation*. *Journal of Applied Electrochemistry*, 2003. **33**(12): p. 1107-1123.

37. Hori, Y., et al., *Production of methane and ethylene in electrochemical reduction of carbon dioxide at copper electrode in aqueous hydrogencarbonate solution*. Chemistry Letters, 1986. **15**(6): p. 897-898.
38. Hansen, H.A., et al., *Understanding trends in the electrocatalytic activity of metals and enzymes for CO₂ reduction to CO*. The journal of physical chemistry letters, 2013. **4**(3): p. 388-392.
39. Kuhl, K.P., et al., *New insights into the electrochemical reduction of carbon dioxide on metallic copper surfaces*. Energy & Environmental Science, 2012. **5**(5): p. 7050-7059.
40. Hori, Y., et al., *Electrocatalytic process of CO selectivity in electrochemical reduction of CO₂ at metal electrodes in aqueous media*. Electrochimica Acta, 1994. **39**(11-12): p. 1833-1839.
41. Aulice Scibioh M., V.B., *Chapter 10 - Perspectives—CO₂ Conversion to Fuels and Chemicals*. Carbon Dioxide to Chemicals and Fuels, 2018: p. 475-482.
42. Wu, J., et al., *Electrochemical reduction of carbon dioxide I. Effects of the electrolyte on the selectivity and activity with Sn electrode*. Journal of the Electrochemical Society, 2012. **159**(7): p. F353.
43. Lv, W., et al., *Studies on the faradaic efficiency for electrochemical reduction of carbon dioxide to formate on tin electrode*. Journal of Power Sources, 2014. **253**: p. 276-281.
44. Lei, F., et al., *Metallic tin quantum sheets confined in graphene toward high-efficiency carbon dioxide electroreduction*. Nature communications, 2016. **7**(1): p. 1-8.
45. Choi, S.Y., et al., *Electrochemical reduction of carbon dioxide to formate on tin-lead alloys*. ACS Sustainable Chemistry & Engineering, 2016. **4**(3): p. 1311-1318.
46. Jiao, F., W. Luc, and M. Jouny. *Bimetallic catalyst with a core-shell structure for CO₂ reduction*. in *ABSTRACTS OF PAPERS OF THE AMERICAN CHEMICAL SOCIETY*. 2018. AMER CHEMICAL SOC 1155 16TH ST, NW, WASHINGTON, DC 20036 USA.
47. Liu, Y., et al., *Design and engineering of urchin-like nanostructured SnO₂ catalysts via controlled facial hydrothermal synthesis for efficient electro-reduction of CO₂*. Electrochimica Acta, 2017. **248**: p. 123-132.
48. Zhao, Y., et al., *Tunable and efficient tin modified nitrogen-doped carbon nanofibers for electrochemical reduction of aqueous carbon dioxide*. Advanced Energy Materials, 2018. **8**(10): p. 1702524.
49. Yadav, V., et al., *Synthesis of Sn catalysts by solar electro-deposition method for electrochemical CO₂ reduction reaction to HCOOH*. Catalysis Today, 2018. **303**: p. 276-281.
50. Choi, Y.-W., et al., *Enhanced Stability and CO/Formate Selectivity of Plasma-Treated SnO_x/AgO_x Catalysts during CO₂ Electroreduction*. Journal of the American Chemical Society, 2019. **141**(13): p. 5261-5266.
51. Li, D., et al., *Tuning the pore structure of porous tin foam electrodes for enhanced electrochemical reduction of carbon dioxide to formate*. Chemical Engineering Journal, 2019. **375**: p. 122024.
52. Li, F., *Efficient electrochemical reduction of CO₂ to formate using Sn-Polyaniline film on Ni foam*. Electrochimica Acta, 2020. **332**: p. 135457.

53. Li, H., et al., *Promoting the electroreduction of CO₂ with oxygen vacancies on a plasma-activated SnO_x/carbon foam monolithic electrode*. Journal of Materials Chemistry A, 2020. **8**(4): p. 1779-1786.
54. Yang, Q., et al., *Novel Bi-Doped Amorphous SnO_x Nanoshells for Efficient Electrochemical CO₂ Reduction into Formate at Low Overpotentials*. Advanced Materials, 2020. **32**(36): p. 2002822.
55. Qian, Y., et al., *Highly efficient electroreduction of CO₂ to formate by nanorod@ 2D nanosheets SnO*. Journal of CO₂ Utilization, 2020. **42**: p. 101287.
56. Chen, G., et al., *Enhanced efficiency for carbon dioxide electroreduction to formate by electrodeposition Sn on Cu nanowires*. Journal of CO₂ Utilization, 2021. **44**: p. 101409.
57. Zhong, H., et al., *Ordered cone-structured tin directly grown on carbon paper as efficient electrocatalyst for CO₂ electrochemical reduction to formate*. Journal of Energy Chemistry, 2021. **55**: p. 236-243.
58. Chen, Y., C.W. Li, and M.W. Kanan, *Aqueous CO₂ reduction at very low overpotential on oxide-derived Au nanoparticles*. Journal of the American Chemical Society, 2012. **134**(49): p. 19969-19972.
59. Hall, A.S., et al., *Mesostructure-induced selectivity in CO₂ reduction catalysis*. Journal of the American Chemical Society, 2015. **137**(47): p. 14834-14837.
60. Chen, C., et al., *Selective electrochemical CO₂ reduction over highly porous gold films*. Journal of Materials Chemistry A, 2017. **5**(41): p. 21955-21964.
61. Andrews, E., Y. Fang, and J. Flake, *Electrochemical reduction of CO₂ at CuAu nanoparticles: size and alloy effects*. Journal of Applied Electrochemistry, 2018. **48**(4): p. 435-441.
62. Yu, J., et al., *When amine-based conducting polymers meet Au nanoparticles: suppressing H₂ evolution and promoting the selective electroreduction of CO₂ to CO at low overpotentials*. Sustainable Energy & Fuels, 2021. **5**(3): p. 779-786.
63. Liu, Z., et al., *Copper decorated with nanoporous gold by galvanic displacement acts as an efficient electrocatalyst for the electrochemical reduction of CO₂*. Nanoscale, 2021. **13**(2): p. 1155-1163.
64. Choi, J., et al., *Electrochemical CO₂ reduction to CO on dendritic Ag–Cu electrocatalysts prepared by electrodeposition*. Chemical Engineering Journal, 2016. **299**: p. 37-44.
65. Park, H., et al., *AgIn dendrite catalysts for electrochemical reduction of CO₂ to CO*. Applied Catalysis B: Environmental, 2017. **219**: p. 123-131.
66. Yu, Y., et al., *Comparative Study between Pristine Ag and Ag Foam for Electrochemical Synthesis of Syngas with Carbon Dioxide and Water*. Catalysts, 2019. **9**(1): p. 57.
67. Qian, Y., et al., *Investigating the Formation Mechanism of a Nanoporous Silver Film Electrode with Enhanced Catalytic Activity for CO₂ Electroreduction*. ChemElectroChem, 2020. **7**(21): p. 4354-4360.
68. Yun, H., et al., *Electrochemical CO₂ reduction to CO on dendritic Ag-Cu electrocatalysts prepared by electrodeposition*. Electrochimica Acta, 2021. **371**.
69. Wang, Y., et al., *Zinc imidazolate metal–organic frameworks (ZIF-8) for electrochemical reduction of CO₂ to CO*. ChemPhysChem, 2017. **18**(22): p. 3142-3147.

70. Zhang, T., et al., *Multilayered Zn nanosheets as an electrocatalyst for efficient electrochemical reduction of CO₂*. *Journal of catalysis*, 2018. **357**: p. 154-162.
71. Luo, W., et al., *Boosting CO production in electrocatalytic CO₂ reduction on highly porous Zn catalysts*. *ACS Catalysis*, 2019. **9**(5): p. 3783-3791.
72. Luo, W., et al., *Electrochemical reconstruction of ZnO for selective reduction of CO₂ to CO*. *Applied Catalysis B: Environmental*, 2020. **273**: p. 119060.
73. Xie, J., Y. Huang, and H. Yu, *Tuning the catalytic selectivity in electrochemical CO₂ reduction on copper oxide-derived nanomaterials*. *Frontiers of Environmental Science & Engineering*, 2015. **9**(5): p. 861-866.
74. Gamburg, Y.D. and G. Zangari, *Introduction to electrodeposition: Basic terms and fundamental concepts*, in *Theory and Practice of Metal Electrodeposition*. 2011, Springer. p. 1-25.
75. Jayakrishnan, D.S., *Electrodeposition: the versatile technique for nanomaterials*, in *Corrosion protection and control using nanomaterials*. 2012, Elsevier. p. 86-125.
76. Alias, N. and A.A. Mohamad, *Morphology study of electrodeposited zinc from zinc sulfate solutions as anode for zinc-air and zinc-carbon batteries*. *Journal of King Saud University-Engineering Sciences*, 2015. **27**(1): p. 43-48.
77. Duan, Z., et al., *An improved model for the calculation of CO₂ solubility in aqueous solutions containing Na⁺, K⁺, Ca²⁺, Mg²⁺, Cl⁻, and SO₄²⁻*. *Marine Chemistry*, 2006. **98**(2-4): p. 131-139.
78. Kaneco, S., et al., *Effect of sodium cation on the electrochemical reduction of CO₂ at a copper electrode in methanol*. *Journal of solid state electrochemistry*, 2007. **11**(4): p. 490-495.
79. Rosen, B.A., et al., *Ionic liquid-mediated selective conversion of CO₂ to CO at low overpotentials*. *Science*, 2011. **334**(6056): p. 643-644.
80. Liu, S., et al., *Rational design of silver sulfide nanowires for efficient CO₂ electroreduction in ionic liquid*. *ACS Catalysis*, 2018. **8**(2): p. 1469-1475.
81. Zhu, Q., et al., *Efficient reduction of CO₂ into formic acid on a lead or tin electrode using an ionic liquid catholyte mixture*. *Angewandte Chemie*, 2016. **128**(31): p. 9158-9162.
82. Singh, M.R., E.L. Clark, and A.T. Bell, *Effects of electrolyte, catalyst, and membrane composition and operating conditions on the performance of solar-driven electrochemical reduction of carbon dioxide*. *Physical Chemistry Chemical Physics*, 2015. **17**(29): p. 18924-18936.
83. S Bello Forero, J., et al., *Propylene carbonate in organic synthesis: exploring its potential as a green solvent*. *Current Organic Synthesis*, 2016. **13**(6): p. 834-846.
84. Shen, F.-x., et al., *Electrochemical reduction of CO₂ to CO over Zn in propylene carbonate/tetrabutylammonium perchlorate*. *Journal of Power Sources*, 2018. **378**: p. 555-561.
85. Ju, F., J. Zhang, and W. Lu, *Efficient Electrochemical Reduction of CO₂ to CO in Ionic Liquid/Propylene Carbonate Electrolyte on Ag Electrode*. *Catalysts*, 2020. **10**(10): p. 1102.
86. Banthia, S., et al., *Substrate effect on electrodeposited copper morphology and crystal shapes*. *Surface Engineering*, 2018. **34**(6): p. 485-492.

87. Wang, R., D. Kirk, and G. Zhang, *Effects of deposition conditions on the morphology of zinc deposits from alkaline zincate solutions*. Journal of The Electrochemical Society, 2006. **153**(5): p. C357.
88. Kuhl, K.P., et al., *Electrocatalytic conversion of carbon dioxide to methane and methanol on transition metal surfaces*. Journal of the American Chemical Society, 2014. **136**(40): p. 14107-14113.
89. Li, G.-R., et al., *Electrochemical self-assembly of ZnO nanoporous structures*. The Journal of Physical Chemistry C, 2007. **111**(5): p. 1919-1923.
90. Sahoo, G.P., et al., *Hydrothermal synthesis of hexagonal ZnO microstructures in HPMC polymer matrix and their catalytic activities*. Journal of Molecular Liquids, 2015. **212**: p. 665-670.
91. Sharma, S., S. Mehta, and S. Kansal, *N doped ZnO/C-dots nanoflowers as visible light driven photocatalyst for the degradation of malachite green dye in aqueous phase*. Journal of Alloys and Compounds, 2017. **699**: p. 323-333.
92. Li, C.W. and M.W. Kanan, *CO₂ reduction at low overpotential on Cu electrodes resulting from the reduction of thick Cu₂O films*. Journal of the American Chemical Society, 2012. **134**(17): p. 7231-7234.
93. Tang, W., et al., *The importance of surface morphology in controlling the selectivity of polycrystalline copper for CO₂ electroreduction*. Physical Chemistry Chemical Physics, 2012. **14**(1): p. 76-81.
94. Rosen, B.A., et al., *In situ spectroscopic examination of a low overpotential pathway for carbon dioxide conversion to carbon monoxide*. The Journal of Physical Chemistry C, 2012. **116**(29): p. 15307-15312.
95. Sun, L., et al., *Switching the reaction course of electrochemical CO₂ reduction with ionic liquids*. Langmuir, 2014. **30**(21): p. 6302-6308.





APPENDIX

จุฬาลงกรณ์มหาวิทยาลัย
CHULALONGKORN UNIVERSITY

APPENDIX A

THE CALIBRATION CURVE OF GAS PRODUCT

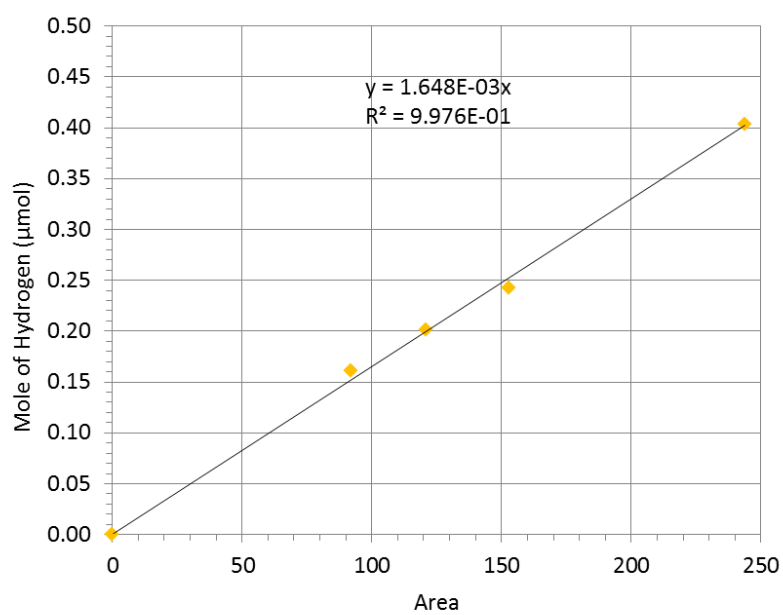
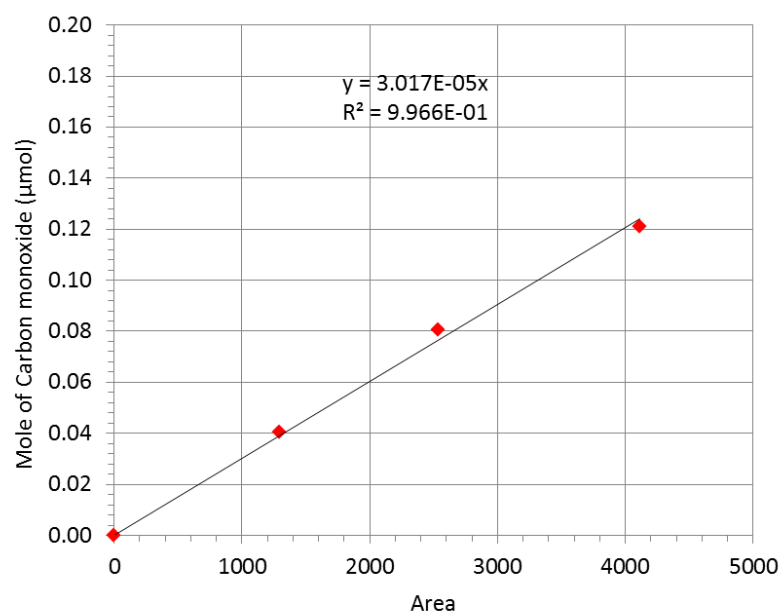
Figure A.1. The calibration curve of H₂.

Figure A.2. The calibration curve of CO.

The calibration curves of H₂ and CO, as shown in Figure A.1 and Figure A.2 were made by injection gas at 3 values in unit of volume via GC. Then, the obtained area of peak in GC will be introduced to plot between volume of gas (x axis) and area of gas (y axis). And finally, an amount gas in unit of volume was converted into unit of mole by use of the ideal gas law equation as shown below

$$PV = nRT$$

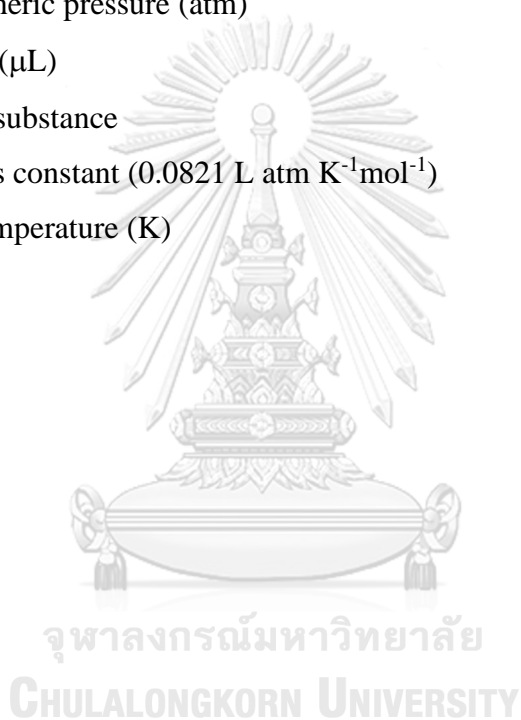
where P is atmospheric pressure (atm)

V is volume (μL)

n is mole of substance

R is ideal gas constant (0.0821 L atm K⁻¹mol⁻¹)

T is room temperature (K)



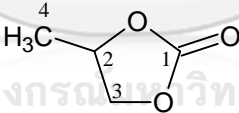
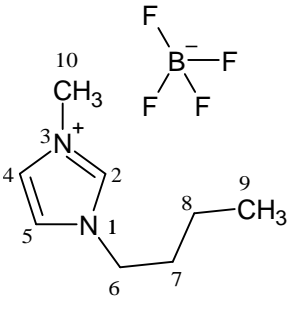
APPENDIX B

THE LIQUID PRODUCT IDENTIFICATION FOR NMR ANALYSIS

Table B.1. ^1H -NMR Spectra of Cathodic Electrolytes (0.1M KHCO_3) in CO_2 Reduction [39].

Product name	^1H splitting	Chemical Shift
Formate	s	8.33
DMSO (Internal Standard)	s	2.6
n-Propanol	t	0.77

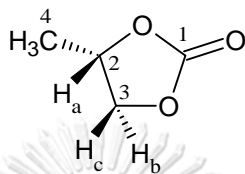
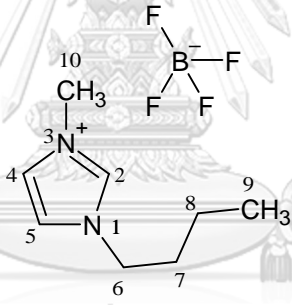
Table B.2. ^{13}C -NMR Spectra of Cathodic Electrolytes (BMIM+PC system) in CO_2 Reduction.

Compounds	Molecular Structure	Chemical Shift (δ ppm)	
		Before Reaction (0 mins)	After Reaction (70 mins)
Propylene carbonate		(C1) 155.37	(C1) 155.64
		(C2) 74.16	(C2) 74.33
		(C3) 70.88	(C3) 70.91
		(C4) 18.95	(C4) 18.80
1-Butyl-3-methylimidazolium tetrafluoroborate		(C2) 136.80	(C2) 136.60
		(C4) 122.52	(C4) 122.30
		(C5) 123.84	(C5) 123.66
		(C6) 48.96	(C6) 49.09
		(C7) 31.73	(C7) 31.61
		(C8) 19.28	(C8) 19.07
	(C9) 13.43	(C9) 13.24	
	(C10) 35.92	(C10) 35.70	

Note: d_6 -DMSO used as solvent

Spectrometer 400 MHz

Table B.3. $^1\text{H-NMR}$ Spectra of Cathodic Electrolytes (BMIM+PC system) in CO_2 Reduction.

Compounds	Molecular Structure	Chemical Shift (δ ppm)	
		Before Reaction (0 mins)	After Reaction (70 mins)
Propylene carbonate		(H2a, 1H, t) 4.88	(H2a, 1H, t) 4.84
		(H3b, 1H, dd) 4.54, $J=8$ Hz	(H3b, 1H, dd) 4.52, $J=8$ Hz
		(H3c, 1H, dd) 4.04, $J=8$ Hz	(H3c, 1H, dd) 4.01, $J=8$ Hz
		(H4, 3H, s) 1.38	(H4, 3H, s) 1.35
1-Butyl-3-methylimidazolium tetrafluoroborate		(H2, 1H, t) 8.96	(H2, 1H, t) 8.76
		(H5, 1H, t) 7.68	(H5, 1H, t) 7.53
		(H4, 1H, t) 7.61	(H4, 1H, t) 7.50
		(H6, 2H, t) 4.14	(H6, 2H, t) 4.09
		(H7, 2H, m) 1.72	(H7, 2H, m) 1.72
		(H8, 2H, m) 1.24	(H8, 2H, m) 1.29
		(H9, 3H, t) 0.87	(H9, 3H, t) 0.83
		(H10, 3H, s) 3.84	(H10, 3H, s) 3.84

Note: d_6 -DMSO used as solvent, s = singlet, dd = doublet of doublet, t = triplet, m = multiplet

Spectrometer 400 MHz

VITA

NAME Krongkwan Poonbun

DATE OF BIRTH 7 November 1996

PLACE OF BIRTH Prachinburi, Thailand

**INSTITUTIONS
ATTENDED** B.Eng Chemical Engineering Faculty of Engineering,
Thammasat University

HOME ADDRESS 237/10 Yinglak Village, Dongpraram District, Prachinburi
Province, 25000



จุฬาลงกรณ์มหาวิทยาลัย
CHULALONGKORN UNIVERSITY